TNPO2 variants associate with human developmental delays, neurologic deficits, and dysmorphic features and alter *TNPO2* activity in *Drosophila*

Lindsey D. Goodman,[1,2] Heidi Cope,[3] Zelha Nil,[1,2] Thomas A. Ravenscroft,[1,2] Wu-Lin Charng,[1,2,31] Shenzhao Lu,[1,2] An-Chi Tien,[1,2,32] Rolph Pfundt,[4] David A. Koolen,[4] Charlotte A. Haaxma,[5] Hermine E. Veenstra-Knol,[6] Jolien S. Klein Wassink-Ruiter,[6] Marijke R. Wevers,[7] Melissa Jones,[8] Laurence E. Walsh,[9] Victoria H. Klee,[9] Miel Theunis,[10] Eric Legius,[11] Dora Steel,[12,13] Katy E.S. Barwick,[12] Manju A. Kurian,[12,13] Shekeeb S. Mohammad,[14,15] Russell C. Dale,[14,15] Paulien A. Terhal,[16]

(Author list continued on next page)

Summary

Transportin-2 (TNPO2) mediates multiple pathways including non-classical nucleocytoplasmic shuttling of >60 cargoes, such as developmental and neuronal proteins. We identified 15 individuals carrying *de novo* coding variants in *TNPO2* who presented with global developmental delay (GDD), dysmorphic features, ophthalmologic abnormalities, and neurological features. To assess the nature of these variants, functional studies were performed in *Drosophila*. We found that fly *dTnpo* (orthologous to *TNPO2*) is expressed in a subset of neurons. *dTnpo* is critical for neuronal maintenance and function as downregulating *dTnpo* in mature neurons using RNAi disrupts neuronal activity and survival. Altering the activity and expression of *dTnpo* using mutant alleles or RNAi causes developmental defects, including eye and wing deformities and lethality. These effects are dosage dependent as more severe phenotypes are associated with stronger *dTnpo* loss. Interestingly, similar phenotypes are observed with *dTnpo* upregulation and ectopic expression of *TNPO2*, showing that loss and gain of Transportin activity causes developmental defects. Further, proband-associated variants can cause more or less severe developmental abnormalities compared to wild-type *TNPO2* when ectopically expressed. The impact of the variants tested seems to correlate with their position within the protein. Specifically, those that fall within the RAN binding domain cause more severe toxicity and those in the acidic loop are less toxic. Variants within the cargo binding domain show tissue-dependent effects. In summary, *dTnpo* is an essential gene in flies during development and in neurons. Further, proband-associated *de novo* variants within *TNPO2* disrupt the function of the encoded protein. Hence, *TNPO2* variants are causative for neurodevelopmental abnormalities.

Introduction

Genomic sequencing in combination with functional investigations in model organisms has led to the discovery of numerous novel Mendelian diseases.[1,2] Functional investigations may be particularly impactful when considering contributions of potential disease-associated variants that occur in genes encoding pleiotropic proteins,[3,4] defined as proteins that function in a diverse number of unrelated pathways.

Here, we identified *Transportin-2* (*TNPO2* [MIM: 603002]; *Importin-3*; *Karyopherin-β2b*) as a disease-associated gene. TNPO2 primarily mediates a non-classical nucleocytoplasmic shuttling pathway.[5,6] TNPO2 activity is dependent on the Ras-related nuclear protein (RAN) GTP/GDP gradient.[7] During nucleocytoplasmic shuttling, TNPO2 is bound by RAN-GDP at its N terminus, promoting interactions with cytoplasmic protein cargoes at its C terminus.[5,6] Subsequently, the RAN-GDP:TNPO2:cargo complex is shuttled into the nucleus via the nuclear pore complex (NPC). Conversion of RAN-GDP to RAN-GTP in the nucleus causes a conformational change in TNPO2's acidic loop—a flexible domain found between the RAN and cargo binding domains. This releases the cargo. RAN-GTP:TNPO2 is then shuttled back to the cytoplasm, destined to repeat the process.

TNPO2 is closely related to *Transportin-1* (*TNPO1* [MIM: 602901]*; Importin-2; Karyopherin-β2*)[5] and neither gene

[1]Department of Molecular and Human Genetics, Baylor College of Medicine, Houston, TX 77030, USA; [2]Jan and Dan Duncan Neurological Research Institute, Texas Children's Hospital, Houston, TX 77030, USA; [3]Division of Medical Genetics, Department of Pediatrics, Duke University Medical Center, Durham, NC 27710, USA; [4]Department of Human Genetics, Donders Institute for Brain, Cognition and Behaviour, Radboud University Medical Center, Geert Grooteplein Zuid 10, 6525 GA, PO Box 9101, Nijmegen, the Netherlands; [5]Department of Pediatric Neurology, Amalia Children's Hospital, Radboud University Medical Center, Nijmegen, Geert Grooteplein Zuid 10, 6525 GA, PO Box 9101, the Netherlands; [6]Department of Genetics, University of Groningen, University Medical Center Groningen, 9713 GZ Groningen, the Netherlands; [7]Department of Genetics, Radboud University Medical Center, PO Box 9101, 6500 HB Nijmegen, the Netherlands; [8]Houston Area Pediatric Neurology, 24514 Kingsland Blvd, Katy, TX 77494, USA; [9]Department of Pediatric Neurology, Riley Hospital for Children, Indianapolis, IN 46202, USA; [10]Center for Human Genetics, University Hospital Leuven, Herestraat 49, 3000 Leuven, Belgium; [11]Department of Human Genetics, University of Leuven, Herestraat 49, 3000 Leuven, Belgium; [12]Molecular Neurosciences, Developmental Neurosciences, UCL Great Ormond Street Institute of Child Health, London WC1N 1EH, UK; [13]Department of Neurology, Great Ormond Street Hospital, London WC1N 3JH, UK; [14]T.Y. Nelson Department of Neurology and Neurosurgery, The Children's Hospital at Westmead, Westmead, NSW

(Affiliations continued on next page)

Ellen van Binsbergen,[16] Brian Kirmse,[17] Bethany Robinette,[17] Benjamin Cogné,[18,19] Bertrand Isidor,[18,19] Theresa A. Grebe,[20,21] Peggy Kulch,[20] Bryan E. Hainline,[22] Katherine Sapp,[22] Eva Morava,[23,24] Eric W. Klee,[23,24] Erica L. Macke,[23] Pamela Trapane,[25] Christopher Spencer,[25] Yue Si,[26] Amber Begtrup,[26] Matthew J. Moulton,[1,2] Debdeep Dutta,[1,2] Oguz Kanca,[1,2] Undiagnosed Diseases Network,[27] Michael F. Wangler,[1,2] Shinya Yamamoto,[1,2,28,29] Hugo J. Bellen,[1,2,28,29,30,*] and Queenie K.-G. Tan[3,*]

has been associated with a Mendelian disease. *TNPO2* is the less studied of the two as it was discovered later. Human TNPO2 and TNPO1 protein sequences are 84% identical and 92% similar.[5] Differences primarily occur in their flexible acidic loops and, to a lesser extent, their cargo-binding domains.[8] Current data support that TNPO2 and TNPO1 are functionally redundant.[5] Although the two genes are expressed ubiquitously, they differ in their expression levels in different tissues. Expression profiling data in mice demonstrated that *TNPO2* is more highly expressed in the brain than *TNPO1*.[9] These results are consistent with other mammalian datasets.[5] At the protein level, TNPO2 is more abundant in cultured neurons, astrocytes, and neural stem cells than TNPO1.[10] TNPO2 may also be more critical in muscles as TNPO1 is not detected in cultured myoblasts.[11] TNPO2 is required during myoblast differentiation into myotubes.[11]

More than 150 proteins are predicted to interact with TNPO1/2 based on high-throughput studies and more than 60 proteins have been confirmed as TNPO1 cargoes.[5,12,13] Cargoes confirmed to be shuttled by TNPO2 include FUS (MIM: 137070),[14] HuR/ElavL1 (MIM: 603466),[8,11,15,16] hnRNPA1 (MIM: 164017),[8,17] and NF-κB Essential Modulator (NEMO [MIM: 300248]).[18] All of these are also TNPO1 cargoes. Recent high-throughput studies have detected rare proteins that uniquely interact with TNPO2[12,13] but direct investigations are needed to confirm them as TNPO2-specific cargoes.

The majority of TNPO1/2 cargoes carry a non-canonical nuclear-localization signal (NLS), a PY-NLS, defined as a C-terminal R/H/K-$X_{2\text{-}5}$PY motif.[17] However, a large number of cargoes do not have a PY-NLS and are simply described as being structurally disordered and having a hydrophobic or basic N-terminal sequence.[5,19] RNA-binding proteins and transcription factors needing import into the nucleus to regulate expression of a diverse number of genes are common targets of TNPO1/2[5]. Other nucleus-bound cargoes include histones, splicing factors, and ribosomal proteins.[5,12,13] TNPO1/2 also interacts with ciliary proteins,[20–22] spindle assembly factors,[23,24] and nucleoporins,[23,25,26] shuttling these cargoes to the appropriate region of the cell for them to function. This means TNPO1/2 activity directly impacts ciliogenesis, mitotic spindle assembly, and nuclear envelope and pore assembly. Last, TNPO1/2 has been implicated in mechanisms that promote aging and neurodegenerative diseases.[14,27–29]

Here we characterize a cohort that carry *de novo* variants within *TNPO2*, finding that common features include developmental and neurological abnormalities. Using *Drosophila* to perform functional studies, we provide evidence that *de novo,* pathogenic variants in *TNPO2* are the genetic causes of individuals' symptoms.

Material and methods

Recruitment and sequencing of individuals

Fifteen individuals were recruited through the Undiagnosed Diseases Network (UDN)[30] and GeneMatcher.[31] The procedures followed were in accordance with the ethical standards of the responsible committee on human experimentation (institutional and national). Proper informed consent was obtained from family members for all probands in this study. All of the UDN work, including clinical and model organism work, and coordination for this publication, was performed under NIH IRB protocol 15-HG-0130.

Sequencing details for each proband can be found in Data S1. Briefly, trio (proband and both biological parents) whole-exome sequencing (WES) was done in 14 of 15 affected individuals as previously described.[32–34] Trio whole-genome sequencing (WGS) used the Illumina Novaseq 6000 platform. Sequencing libraries were generated using the Truseq Nano DNA HT Sample Preparation Kit (Illumina). Alignment of 150 bp paired-end reads to the hg19 reference genome was performed using Burrows-Wheeler Aligner (BWA) software, before sorting with samtools and marking duplicates with Picard. Single-nucleotide variants (SNVs) and small insertions/deletions (indels) were labeled using Genome Analysis Tool Kit (GATK v.3.1), structural variants (SVs) were

2145, Australia; [15]Kids Neuroscience Centre, The Children's Hospital at Westmead, Faculty of Medicine and Health, Sydney Medical School, University of Sydney, Sydney, Westmead, NSW 2145, Australia; [16]Department of Genetics, University Medical Center Utrecht, Lundlaan 6, 3584 EA Utrecht, the Netherlands; [17]Department of Pediatrics, University of Mississippi Medical Center, Jackson, MS 39216, USA; [18]Centre hospitalier universitaire (CHU) de Nantes, Service de Génétique Médicale, 9 quai Moncousu, 44093 Nantes, France; [19]INSERM, CNRS, UNIV Nantes, Centre hospitalier universitaire (CHU) de Nantes, l'institut du thorax, 44007 Nantes, France; [20]Phoenix Children's Hospital, Phoenix, AZ 85016, USA; [21]Department of Child Health, University of Arizona College of Medicine Phoenix, Phoenix, AZ 85004, USA; [22]Medical and Molecular Genetics, Indiana University School of Medicine, Indianapolis, IN 46202, USA; [23]Center for Individualized Medicine, Mayo Clinic, Rochester, MN 55905, USA; [24]Department of Clinical Genomics, Mayo Clinic, Rochester, MN 55905, USA; [25]University of Florida, College of Medicine, Jacksonville, Jacksonville, FL 32209, USA; [26]GeneDx, Gaithersburg, MD 20877, USA; [27]The Undiagnosed Diseases Network (UDN) consortia, see Supplemental Note S2 for co-investigators, Harvard University, Cambridge, MA 02138, USA; [28]Department of Neuroscience, Baylor College of Medicine, Houston, TX 77030, USA; [29]Development, Disease Models & Therapeutics Graduate Program, Baylor College of Medicine, Houston, TX 77030, USA; [30]Howard Hughes Medical Institute, Baylor College of Medicine, Houston, TX 77030, USA
[31]Present address: Department of Neurology, Washington University in St. Louis, St. Louis, MO 63110, USA
[32]Present address: Ivy Brain Tumor Center, Barrow Neurological Institute, Phoenix, AZ 85013, USA
*Correspondence: hbellen@bcm.edu (H.J.B.), khoon.tan@duke.edu (Q.K.-G.T.)
https://doi.org/10.1016/j.ajhg.2021.06.019.

detected using DELLY (v0.7.3) software, and copy number variants (CNVs) were detected using the control-FREEC (v.9.9) tool. Following genomic variants detection, variants were annotated using ANNOVAR. Identification of genomic regions affected by each variant and possible changes in protein was performed using RefSeq and Gencode databases. The presence of the variants were assessed in dbSNP, GnomAD, 1000 Genomes Project, Exome Aggregation Consortium (ExAC), exome sequencing project (ESP), and Clinvar. Databases dbSNP, COSMIC, OMIM, GWAS Catalog, and HGMD were used to find reported information of variants. SIFT, PolyPhen, MutationAssessor, LRT, and CADD scores were used to predict the deleteriousness of mutations and GERP++ scores were used to access the conservation of mutations.

Drosophila husbandry and established fly lines

All fly lines were raised and maintained as described.[35] Publicly available fly lines are detailed in Table S1 and were obtained from Vienna *Drosophila* Research Center (VDRC), Bloomington *Drosophila* Stock Center (BDSC), and Kyoto Stock Center (Kyoto). *Rh1-GAL4* on II (*w*; Rh1-GAL4;*), *elav-GAL4* on II (*y* w*; elav-GAL4*) and *UAS-(empty)* control (*y w; PBac{UAS-empty}VK37/SM6a*) were published previously.[36,37] *da-GAL4^{GS}* (*w*; P{da-GSGAL4.T};*) was generously provided by H. Tricoire.[38]

dTnpo mutant alleles and genomic rescue line

dTnpo^{Gly736Asp}, *Tnpo-RA* (GenBank: NM_058020.4):*c.2207G>A (p.Gly736Asp)*, was identified in a forward genetic screen of *FRT80B* isogenized flies.[39] *dTnpo$^{\Delta 11}$* is an imprecise excision line derived from *P{GawB}NP4408*[40] (Kyoto #104668). A *dTnpo* genomic rescue construct, *GR^{dTnpo}*, was cloned from the endogenous *dTnpo* loci using genomic DNA from isogenized *FRT80B* and inserted into the VK37 docking site using ϕC31-mediated transgenesis as described.[41] The *dTnpo CRIMIC (T2A-GAL4)* allele was designed as part of the Gene Disruption Project (construct CR92235) as described[42] using sgRNA 5′-CAAGCGTAATTTAA GAGTAATGG-3′.

UAS-hTNPO2 lines

UAS-hTNPO2 lines were developed as described.[35] Q5 site directed mutagenesis (NEB # E00554S) was done on a pDONR223-hTNPO2 cDNA construct (GenBank: NM_001136196.1; Horizon Discovery # OHS1770-202312693) to introduce a stop codon and variants. Primers are detailed in Table S2. LR clonase II (ThermoFisher # 11791020) was used to transfer the cDNA sequence to a pGW-attB-3xHA destination vector,[43] creating pGW-hTNPO2 constructs. All clones were PCR and sequence confirmed. Sequencing primers included ones specific to the *hTNPO2* sequence (Table S2) and M13 primers. pGW-hTNPO2 constructs were inserted into the VK37 docking site using ϕC31-mediated transgenesis.[41] Final genotype: *w^{1118}; PBac{UAS-hTNPO2}VK37/SM6a*.

GeneSwitch-driven transgene expression and lifespan

da-GAL4^{GS} and *elav-GAL4^{GS}* assays were performed as previously described[44] with the following changes. At 1–2 day post-eclosion, animals were placed onto 300 μM for *elav-GAL4^{GS}* or 500 μM for *da-GAL4^{GS}* RU486-containing food. RU486-food was prepared by mixing molten (60°C–65°C) food with 10 mM RU486 (Sigma #M8046; prepared using 200 pf ethanol) to the desired concentration at 2 mL per vial. Molten food was solidified for 1–24 h in a fume hood. For *elav-GAL4^{GS}* lifespan assays, female flies were maintained at 29°C. For *da-GAL4^{GS}* studies, female flies were maintained for 4 days on RU486 at 25°C.

Quantitative real-time polymerase chain reactions (qPCR)

qPCR was performed as previously described[44] with the following changes. The iScript gDNA Clear cDNA Synthesis Kit (BioRad #1725034), iTaq Universal SYBR Green Master Mix (BioRad #1725120), and a BioRad C1000 Touch Cycler were used. Multiple housekeeping genes (*RP49*, *RPS20*, and *Tubulin*) were included for normalizing the data. qPCR primers are described in Table S2 and those for housekeeping genes were previously published.[44]

Immunofluorescence (IF) and confocal microscopy

IF for L3 larval CNS and adult brains was performed as described.[45,46] Primary antibodies: anti-FasII (DSHB #7G10; 1:100), anti-Elav (DSHB #7E8A10; 1:500), anti-Repo (DSHB #8D12; 1:60), anti-mCherry (Genetex # GTX59788; 1:200; also targets RFP). Goat-derived secondary antibodies were used at 1:500 (Jackson ImmunoResearch Laboratories). A Leica Sp8x with lightning deconvolution was used for confocal microscopy. Images were taken with a 20× oil immersion Leica objective (HC PL APO 20x/0.75 IMM CORR CS2).

Western immunoblots (WBs)

The BioRad Mini-PROTEAN Electrophoresis System was used with 4%–20% Mini-PROTEAN TGX Precast Gel (BioRad #4561095), 1× Tris/Glycine/SDS running buffer, 1× Tris/Glycine transfer buffer with 10% methanol, and PVDF membrane. For lysates, whole frozen flies were homogenized as described[44,47] into 1× SDS sample buffer at 50 μL per animal. For 1× SDS sample buffer, 60 μL of β-mercaptoethanol was added to 1 mL of diluted 6× SDS sample buffer (0.35M Tris-HCl [pH 6.8], 10% SDS, 30% glycerol, 30% β-mercaptoethanol, 1% Bromophenol Blue). 10 μL of lysate was loaded per lane. Membranes were stained and reprobed as described.[44,47] Antibodies: anti-hTNPO1/2[A11] (1:1,000, Santa Cruz #sc-365179), anti-mouse-HRP (1:5,000), and anti-α-Tubulin [11H10]-HRP (1:2,000, Cell Signaling #9099). HRP activity was measured using SuperSignal West Pico PLUS Chemiluminescent Substrate (Thermo Sci #34577) and a BioRad Chemidoc MP Imaging System.

Results

Coding variants in *TNPO2* are associated with global developmental delay, dysmorphic features, ophthalmologic abnormalities, and neurological features

Fifteen individuals who primarily presented with feeding difficulties and developmental delays during infancy or in early childhood were evaluated clinically by their providers in the respective institution (Data S1). Trio (proband and both biological parents) sequencing, primarily whole-exome sequencing (WES), was performed by these clinical sites and results showed that these individuals carry a potentially pathogenic, heterozygous coding-variant in *TNPO2* (GenBank: NM_001136196.1) (Table 1; extended data in Data S1). Based on the presence of this variant, individuals were recruited to this study through the

Table 1. Individuals with *TNPO2* variants present with developmental delays, intellectual disability, behavioral deficits, and strabismus

		Proband														
	Summary	1	2	3	4	5	6	7	8	9	10	11	12	13	14	15
Protein variant (p.)	SNV, del, delins	Gln28Arg	Gln32Arg	Pro61Arg	Lys118Asn	Lys152del, mosaic (16/21%)	Asp156Asn	Trp370Arg	Trp370Cys	Lys491_Arg492delinsGlnTrp	Pro514Leu	Ala546Val	Ser548Phe	Phe598Leu	Ala649_Leu652del	Trp727Cys
CADD score	22.7–34.0	27.8	24.3	23.9	22.7	–	27.1	34.0	28.8	–	30.0	27.0	31.0	29.4	–	25.5
Sanger confirmed?	10 of 15	yes	yes	–	yes	yes	–	yes	yes	yes	–	yes	–	yes	–	yes
Inheritance	*de novo*	*de novo*	*de novo*	*de novo*	*de novo*	*de novo*	*de novo*	*de novo*	*de novo*	*de novo*	*de novo*	*de novo*	*de novo*	mother, mosaic (1%)	*de novo*	*de novo*
Additional variants of uncertain significance	6 of 15	–	–	–	–	SETBP1:p.Leu1522Argfs*59; CUX2: p.His1253Pro; 12q13.13_dup	ANKFY1: p.Thr1088Serfs*9	–	ARMC9: p.Asp330Asn	–	1q21.1_ins522Kb	–	–	–	PDE4D: p.Arg237*	INA p.Leu376Pro, mosaic (20%)
Age at onset	neo-18mo	1mo	4mo	neonat.	13mo	3mo	6mo	4mo	neonatal	prenatal	9mo	8mo	neonat.	15mo	18mo	neonat.
Age at exam	14mo-20y	6y	18mo	6mo	3y	23mo	4y	10y	8y	14mo	5y	9y	20y	11y	12y	7y
Global developmental delays	15 of 15	++	+, regress.	+	++, regress.	+++	++	+++	+	+	++	+	+++	+, regress.	+	++
Speech impaired	15 of 15	++	+	+	++	+++	+++	+++	+	+	++	+	+++	+	+	++
Intellectual disability	9 of 9	+++	ND	ND	+++	ND	++	+++	++	ND	ND	++	+++	+	++	ND
Motor Impaired	15 of 15	+	+	+	++	+++	++	+++	+	+	+	+	+++	+	+	+
Dysmorphic features	11 of 15	+	–	+	+	–	+	–	+	+	+	–	+	+	+	+
Behavioral deficits	10 of 14	+	+	+	+	–	+	–	+	–	–	+	ND	+	+	+
GI / feeding abnormalities	11 of 15	+	+	+	–	+	–	+	+	–	+	–	+	+	+	+
Ophthalmologic abnormalities	10 of 15	+	–	–	+	+	+	–	+	+	+	+	–	+	–	+
Muscle tone abnormalities	11 of 15	+, hypo	–	+, hypo	–	+, hypo	+, variable	+, hypo	–	+, hypo	+, variable	–	+, hypo	+, hypo	+, hypo	+, hyper

(*Continued on next page*)

Table 1. *Continued*

	Summary	Proband 1	2	3	4	5	6	7	8	9	10	11	12	13	14	15
Movement / neurological disorder	6 of 15	+	–	–	–	+	+	–	–	–	–	+	+	+	–	-
Seizures	6 of 15	+, febrile	–	–	–	–	+, febrile to non-febrile	+, febrile to non-febrile	–	–	+, febrile to non-febrile	+, febrile to non-febrile	+	–	–	–
Microcephaly	5 of 15	+	–	–	+	+	+	–	–	+	–	–	–	–	–	–
MRI brain abnormalities	7 of 13	–	ND	+	–	+	+	–	+	+	+	–	+	–	ND	–

misZ for *TNPO2* loss is 5.88 (o/e = 0.28). pLI for *TNPO2* loss is 1.00 (o/e = 0.04). *TNPO2* coding DNA (GenBank: NM_001136196.1). All individuals are heterozygous for variants. No variants are found in control genetic databases. See Data S1 and Note S1 for additional details on probands' features and additional variants of uncertain significance. ND, no data; CADD, combined annotation dependent depletion.

Undiagnosed Diseases Network (UDN)[44] and GeneMatcher,[45] independent of their respective clinical features.

All variants are *de novo* except the one in proband 13, whose mother was low-level mosaic. The variant is in 1% of NGS reads in the mother by WES. To learn more about *TNPO2* and potential impact of these variants, we used information accumulated into the Model organism Aggregated Resources or Rare Variant ExpLoration (MARRVEL) tool, v.2.[48] MARRVEL is a valuable resource that brings together multiple sources of information for the investigation of human and model organism based disease research. Here, we found that *TNPO2* is highly constrained, having a missense constraint (misZ) score[49] of 5.88 (observed/expected (o/e) = 0.28) and a probability of loss-of-function intolerance (pLI) score[49,50] of 1.00 (o/e = 0.04) based on gnomAD (genome Aggregation Database), v.2.1.1.[51] Twelve probands carry single-nucleotide variants (SNVs) in *TNPO2* that are predicted to be deleterious using combined annotation dependent depletion (CADD) scores (phred > 20), v.1.4.[52] Proband 5 carries a mosaic, in-frame deletion of p.Lys152del (16% by Sanger, 21% by WGS of reads, DNA from blood). Proband 9 carries a deletion-insertion of p.Lys491_Arg492delinsGlnTrp. Proband 14 carries an in-frame deletion of p.Ala649_Leu652, removing four codons. None of these variants are found in genetic databases containing control populations, including information in gnomAD.[51]

To evaluate common features among probands, information was extracted from chart review as well as clinic visits at the respective institutions. We found that all probands present with global developmental delay (GDD), with either slow or plateaued developmental progress (Tables 1 and S1). Probands 2, 4, and 13 show regression of milestones, mostly transiently. All probands have delayed speech, with expressive language more severely impacted compared with receptive speech. Four individuals are nonverbal (+++) including proband 7 at age 10 years and proband 12 at age 20 years. Motor impairments appear to be comparatively less severe in our cohort compared with speech delays, although probands 5, 7, and 12 are non-ambulatory (+++). Intellectual disability (ID) was assessed and found in nine probands, ranging from mild (+) to severe (+++). ID is also suspected in another three individuals.

Behavioral deficits are observed in 10 of 14 probands with variable presentation (Tables 1 and S1). The most common neuropsychiatric concerns are inattention and autistic behaviors. Proband 12 is severely delayed so behavioral analysis was not done.

Gastrointestinal (GI) features appear to be shared within the cohort, impacting 11 of 15 probands (Tables 1 and S1). The most common features include neonatal feeding difficulties and poor weight gain.

No single craniofacial dysmorphism is reported across the cohort, although dysmorphic features are noted in

Figure 1. TNPO2 variants are associated with varied dysmorphic features in individuals

(A) Proband 4 at age 3 years with short philtrum, broad nasal bridge, large fleshy ears, and coarse facial features.

(B) Proband 8 at age 8 years with strabismus, high nasal bridge, eversion of the lower lip, and clinodactyly.

(C) Proband 11 at age 9 years has no clear dysmorphism.

(D) Proband 13 at age 11 years with deep set eyes and large cupped ears.

11 of 15 individuals (Figure 1; Tables 1 and S1). The most common abnormalities include a broad or high nasal bridge, retrognathia, and a shortened philtrum. Skull and facial features include dolichocephaly, bitemporal narrowing or narrow face/high arched palate in four probands, and microcephaly (defined as less than –2 standard deviations; SD) in five probands. Noticeably, dysmorphisms surrounding the eye area are observed in five probands although presentation varies. This includes deep-set eyes and palpebral fissure length, spacing, or slant irregularities. Dysmorphic ears are also noted in six probands.

Ophthalmologic abnormalities are reported within the cohort and impact 10 of 15 individuals (Tables 1 and S1). Strabismus is observed in seven probands. Saccadic and rapid eye movements are noted in three individuals, resolving in proband 5 by age 23 months. Myopia, hyperopia, or astigmatism are described in four probands.

Muscle tone abnormalities are described in 11 of 15 individuals, primarily hypotonia. Interestingly, probands 6 and 10 show signs of both hypertonia and hypotonia. In addition, movement and neurological disorders, primarily tremors and ataxia, were seen in 6 of 15 probands.

Neurologic impairments are detected in some probands (Tables 1 and S1). Of the 15 individuals, 6 had seizures starting between 1 and 2.5 years of age. Initial presentation in five of these individuals was febrile induced and in four of five, individuals developed non-febrile seizures. Electroencephalograms (EEGs) were abnormal in three of ten probands assessed, with proband 7 showing severe abnormalities consistent with epileptic encephalopathy. Magnetic resonance imaging (MRI) of the brain was done on 13 probands and cerebellar hypoplasia or dysplasia were seen in three probands. *Tnpo2* is highly expressed in this region in mice.[53] Other findings include white matter loss, mild ventricular dilation, hypoplastic caudate nuclei, thin corpus callosum, as well as minor anomalies such as cavum septum pellucidum, enlarged Virchow Robin spaces, and borderline delay in myelination.

Other, less common features for individuals are also observed. This includes renal abnormalities (bilateral pyeloureteral junction stenosis requiring surgery at age 3 months in proband 4, left kidney agenesis in proband 8, and kidney stones in proband 12), nipple abnormalities, cardiac abnormalities (patent ductus arteriosus requiring transcatheter closure in proband 7, mild dilation of the

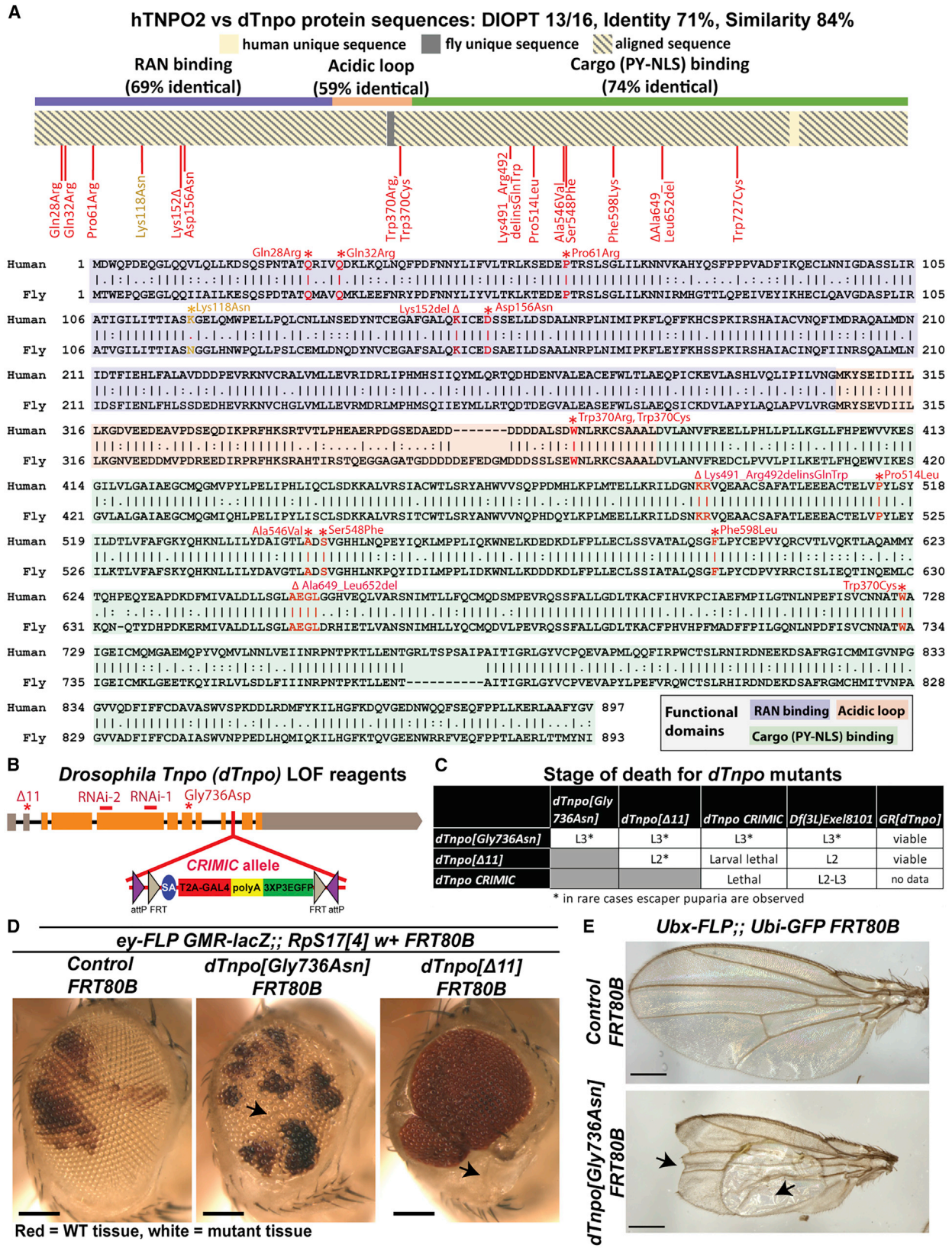

Figure 2. Fly *Transportin* is essential for proper animal development and *dTnpo* loss in eyes and wings causes dysmorphisms
(A) Protein sequence comparison of human TNPO2 (hTNPO2) and *Drosophila* Tnpo (dTnpo) shown as a diagram and a detailed amino acid alignment. All variants are at conserved amino acids (red) except p.Lys118Asn (orange). Symbols in the protein alignment: identical (|), similar (:), different (.), absent (_).

(legend continued on next page)

aortic root in proband 12), finger anomalies, hip dysplasia, (kypho)scoliosis, and pes planus (Data S1).

Of 15 probands, 6 carry additional heterozygous, *de novo* genomic alterations (variants of uncertain significance; VUSs) which were not the primary candidate for further investigation (detailed in Note S1). Briefly, probands 6, 8, and 15 carry SNVs in *Rabankyrin-5* (*ANKFY1* [MIM: 607927]; no disease association), *Armadillo repeat containing 9* (*ARMC9* [MIM: 617612]; associated with autosomal-recessive Joubert syndrome 30 [MIM: 617622]), and *α-Internexin* (*INA* [MIM: 605338]; no disease association), respectively. Importantly, these genes are less constrained than *TNPO2* (see Note S1). Proband 5 carries three VUSs in addition to the one in *TNPO2*. Two are not predicted to be pathogenic based on CADD and other information (see Note S1), including a SNV in *Cut-like Homeobox 2* (*CUX2* [MIM: 610648]; associated with autosomal-dominant developmental and epileptic encephalopathy 67 [MIM: 618141]) and a duplication of 12q13.13. The third is a a deletion-insertion in *SET binding protein 1* (*SETBP1* [MIM: 611060]) that occurs considerably further down in the gene from known pathogenic variants associated with mental retardation, autosomal dominant 29[54] and this individual has no suggestive features for Schinzel-Giedion syndrome[55] ([MIM: 269150]; autosomal dominant). Proband 10 carries multiple VUSs (see Note S1), most notably a 522 Kb gain in 1q21.1. No impacted genes were thought to explain the individual's features. Proband 14 carries a truncating SNV in the highly constrained gene *Phosphodiesterase-4D* (*PDE4D* [MIM: 600129]) and is diagnosed with acrodysostosis 2[56] (ACRDYS2 [MIM: 614613]).

In summary, 15 individuals were identified who carry potential disease-causing variants in *TNPO2*. All individuals present with global developmental delays. Speech abilities and intelligence are typically more impaired than motor abilities. Other common features between probands include variable dysmorphic features, ophthalmologic abnormalities (primarily strabismus), muscle tone abnormalities (primarily hypotonia), movement/neurological disorders, and neurological features.

Drosophila Tnpo is orthologous to human TNPO2 and most proband variants affect evolutionarily conserved residues

To investigate whether the *TNPO2* variants identified in our cohort underlie individuals' features, we utilized the model organism, *Drosophila melanogaster*. The fly ortholog to human *TNPO2* (*hTNPO2*) is *Drosophila Tnpo* (*dTnpo*) and the encoded proteins from these two genes shuttle the same cargoes into the nucleus.[57–61] The amino acid sequences encoded by these two genes are 71% identical and 84% similar (Figure 2A). The DRSC Integrative Ortholog Prediction Tool (DIOPT, v.7.1)[62] score between these genes is 13 of 16, giving strong confidence that *dTnpo* is indeed orthologous to *hTNPO2*. The sequences of the RAN binding and cargo binding domains are more conserved than that of the acidic loop. Specifically, sequences encoding the acidic loops are 59% identical and 70% similar compared to the RAN binding domain (69% identical, 84% similar) and cargo binding domain (74% identical, 85% similar).[8] dTnpo is also orthologous to human TNPO1 (DIOPT score = 13/16), so one fly gene corresponds to two human genes.

Of 15 variants found within our cohort, 14 occur at conserved amino acids between hTNPO2 and dTnpo (Figure 2A, red). Five variants are within the RAN binding domain. Two variants are at the same position within the acidic loop. Seven variants localize to the cargo binding domain. The p.Lys118Asn variant associated with proband 4 is not at a conserved amino acid (Figure 2A, orange) and the amino acid within the fly protein is an asparagine (Asn). This variant is at a conserved amino acid in vertebrate models (see data in MARRVEL).

Developmental loss of *dTnpo* causes lethality and morphologic defects

To gain an understanding of whether *hTNPO2* may be essential during development, we assessed phenotypes associated with *dTnpo* loss in the fly. For this purpose, three *dTnpo* loss-of-function (LoF) mutant alleles were generated using different strategies (Figure 2B). First, we previously identified $dTnpo^{Gly736Asp}$ in a genetic screen.[39] Second, a truncated *dTnpo* mutant, $dTnpo^{\Delta 11}$, was generated by an imprecise excision of a P-element. Last, a *CRISPR-Mediated Integration Cassette (CRIMIC)* allele was created by insertion of a *Splice Acceptor-T2A-GAL4-polyA* sequence into a shared intron of all *dTnpo* transcripts, effectively disrupting the gene's expression by creating a truncated mRNA.[42] We also obtained two available *UAS-RNAi* fly lines designed to target *dTnpo*[63,64] (Figure 2B). These RNAi lines effectively reduce expression of *dTnpo* based on qPCR. *dTnpo* RNAi-1 causes an 81% ± 0.05% reduction and *dTnpo*

(B) *dTnpo* mutants (red) created for loss-of-function (LoF) studies include $dTnpo^{\Delta 11}$ (an imprecise excision of the P-element, *NP4408*), $dTnpo^{Gly736Asp}$ (an EMS-induced mutation), and a *CRIMIC* allele. Two independent RNAi lines, RNAi-1 and RNAi-2, were also obtained.
(C) Animals homozygous for *dTnpo* mutant alleles demonstrate larval lethality due to *dTnpo* loss. None of the alleles or a large deficiency allele which lacks *dTnpo*, *Df(3L)Exel8101*, complement each other. Lethality caused by $dTnpo^{\Delta 11}$ and $dTnpo^{Gly736Asp}$ can be rescued using a genomic rescue construct, GR^{dTnpo}.
(D) The FRT/FLP system was used to make mosaic tissue in the fly eye during development. $dTnpo^{Gly736Asp}$ causes a rough eye phenotype. No homozygous $dTnpo^{\Delta 11}$ mutant tissue is observed, indicating cell lethality. Scale bar = 100 μm.
(E) The FRT/FLP system was used to make mosaic tissue in the developing wing. $dTnpo^{Gly736Asp}$ causes notch and blister phenotypes. Scale bar = 200 μm.
In (D) and (E), "Control" is *yw;; FRT80B*. Full fly genotypes for this and following figures are in Data S2. *dTnpo*-targeting RNAi produce consistent phenotypes (see Figure S1).

RNAi-2 (previously used in Shi et al.[60]) causes a 58% ± 0.16% reduction of *dTnpo* mRNA compared to control RNAi expressing animals (Figure S1A).

The three *dTnpo* mutant alleles are homozygous lethal and no obvious phenotypes are observed in heterozygous animals. Notably, homozygous mutant animals do not survive beyond larval stages of development, shown in Figure 2C. In rare cases, escaper puparia could be observed in $dTnpo^{Gly736Asp}$ cultures and, less commonly, in $dTnpo^{\Delta 11}$ cultures. Based on a complementation test with a deletion line that lacks *dTnpo*, *Df(3L)Exel8101*, we conclude that $dTnpo^{\Delta 11}$ is the most severe LoF allele, causing lethality at larval stage 2 (L2). $dTnpo^{Gly736Asp}$ behaves as a hypomorph based on complementation failure with *Df(3L)Exel8101,* causing death in larval stage 3 (L3). Finally, the *dTnpo CRIMIC* allele also behaves as a hypomorph, causing lethality between L2 and L3. The $dTnpo^{\Delta 11}$ and $dTnpo^{Gly736Asp}$ alleles are rescuable by a genomic rescue line, GR^{dTnpo}, which carries an independent copy of the *dTnpo* loci. Consistent with these data, ubiquitous expression of the strong *UAS-dTnpo RNAi-1* using *da-GAL4* causes lethality at L2, similar to $dTnpo^{\Delta 11}$ mutants (Figure S1B). Further, *da-GAL4* driven expression of the weaker *UAS-dTnpo RNAi-2* causes lethality at L3, similar to $dTnpo^{Gly736Asp}$. Overall, these data show that *dTnpo* is essential during fly development.

Since *hTNPO2* is likely required in multiple tissues and probands with *hTNPO2* coding variants have diverse features, we assessed whether *dTnpo* loss impacts different tissues. Given that the majority of our cohort have ophthalmologic abnormalities, we first focused on the fly eye. The formation of this tissue is well studied and the developmental pathways required for proper eye formation are conserved.[65] The mutant alleles $dTnpo^{Gly736Asp}$ and $dTnpo^{\Delta 11}$ were recombined onto *FRT80B* chromosomes. Using the FRT/FLP system,[66] we crossed these flies to *ey-FLP GMR-lacZ;; RpS174 w+ FRT80B* to create mosaic eyes that include either homozygous mutant clonal tissue (white) or wild-type clonal tissue (red) (Figure 2D). Compared to *FRT80B* controls, $dTnpo^{Gly736Asp}$ *FRT80B* causes eye deformities, including disorganized ommatidia consistent with a rough eye phenotype and smaller eyes. Interestingly, no homozygous mutant tissue is seen in animals carrying the stronger mutation, $dTnpo^{\Delta 11}$ *FRT80B*, demonstrating that *dTnpo* is essential for eye development. Expression of *dTnpo* RNAi in the developing fly eye using *ey-GAL4* shows consistent results, with the stronger *UAS-dTnpo RNAi-1* causing developmental lethality and the weaker *UAS-dTnpo RNAi-2* causing a rough eye phenotype and small eyes (Figure S1D). Thus, effects of *dTnpo* loss on eye development seem to be dosage dependent. Interestingly, expressing *dTnpo* RNAi with *GMR-GAL4*, which expresses later in eye development, did not cause significant alterations to the external fly eye (Figure S1E). These data argue that *dTnpo* is required during early eye imaginal disc development but do not rule out a requirement at later stages.

We next tested for *dTnpo* requirement during fly wing development, also a well-studied tissue that involves conserved signaling pathways for proper formation.[67,68] We created mosaic tissue in the wing disc of $dTnpo^{Gly736Asp}$ *FRT80B* larvae using *Ubx-FLP;; Ubi-GFP FRT80B*. Interestingly, wing notch phenotypes and large blisters can be observed in $dTnpo^{Gly736Asp}$ mutant animals (Figure 2E). Taking an alternative approach, we used *nub-GAL4* to express *UAS-dTnpo RNAi* in the developing wing disc and partially in the thorax. The stronger RNAi-1 causes lethality, consistent with *dTnpo* being required for development. The weaker RNAi-2 causes severe defects in wing morphology with hardly any wing forming (Figure S1C). Hence, *dTnpo* is required for wing development.

In sum, we found that *dTnpo* is required in multiple fly tissues for proper development using *dTnpo* LOF reagents. Interestingly, *dTnpo* loss was dosage dependent with the stronger mutant allele, $dTnpo^{\Delta 11}$, and the stronger *dTnpo* RNAi, causing more severe defects than other hypomorphic reagents.

dTnpo is expressed primarily in neurons of the fly CNS

Given that the majority of the *hTNPO2* cohort have features commonly associated with neurologic deficits and *TNPO2* is highly expressed in the mammalian brain,[9,10] we explored the importance of *dTnpo* in this tissue. First, we defined *dTnpo*'s expression pattern in the L3 larval central nervous system (CNS) and the adult fly brain (Figure 3). The *dTnpo CRIMIC* allele (see Figure 2B) carries a *T2A-GAL4* sequence that expresses a GAL4 transcription factor under control of *dTnpo's* regulatory elements.[42] This GAL4 can drive expression of any *UAS-transgene* in the same spatial and temporal pattern as *dTnpo*.[69] Thus, we used the *dTnpo CRIMIC* allele to express *UAS-mCherry.NLS* (mCherry fluorescent protein localized to the nucleus) (Figures 3A–3L). In larvae, mCherry (*dTnpo*) staining is most common in the central brain, including the cell bodies of mushroom body (MB) neurons, and ventral nerve cord (VNC; corresponding to the mammalian spinal cord) (Figures 3A and 3G); a schematic of the larval CNS is shown in Figure 3S for reference. These are areas that harbor a high density of active neurons at this stage.[70] In adults, mCherry (*dTnpo*) staining shows the highest density in the optic lobe, MB cell bodies, and the central complex (Figures 3D and 3J); a schematic of the adult brain is shown in Figure 3T for reference.

To define localization to specific cell types, the tissue were counterstained with Elav (predominantly marks neurons) or Repo (predominantly marks glia except midline glia).[71–73] In both the larval CNS (Figures 3B and 3C) and adult brain (Figures 3E and 3F), not all Elav-positive cells stain positive for mCherry (*dTnpo*) in whole-mount, Z stacked images, supporting that *dTnpo* is expressed in a subset of neurons. These findings were consistent when using single-slice images of regions that show high mCherry staining in both the larval CNS (Figures 3A′–3C′) and adult brain (Figures 3D′–3F′). In whole mount with Z stacked

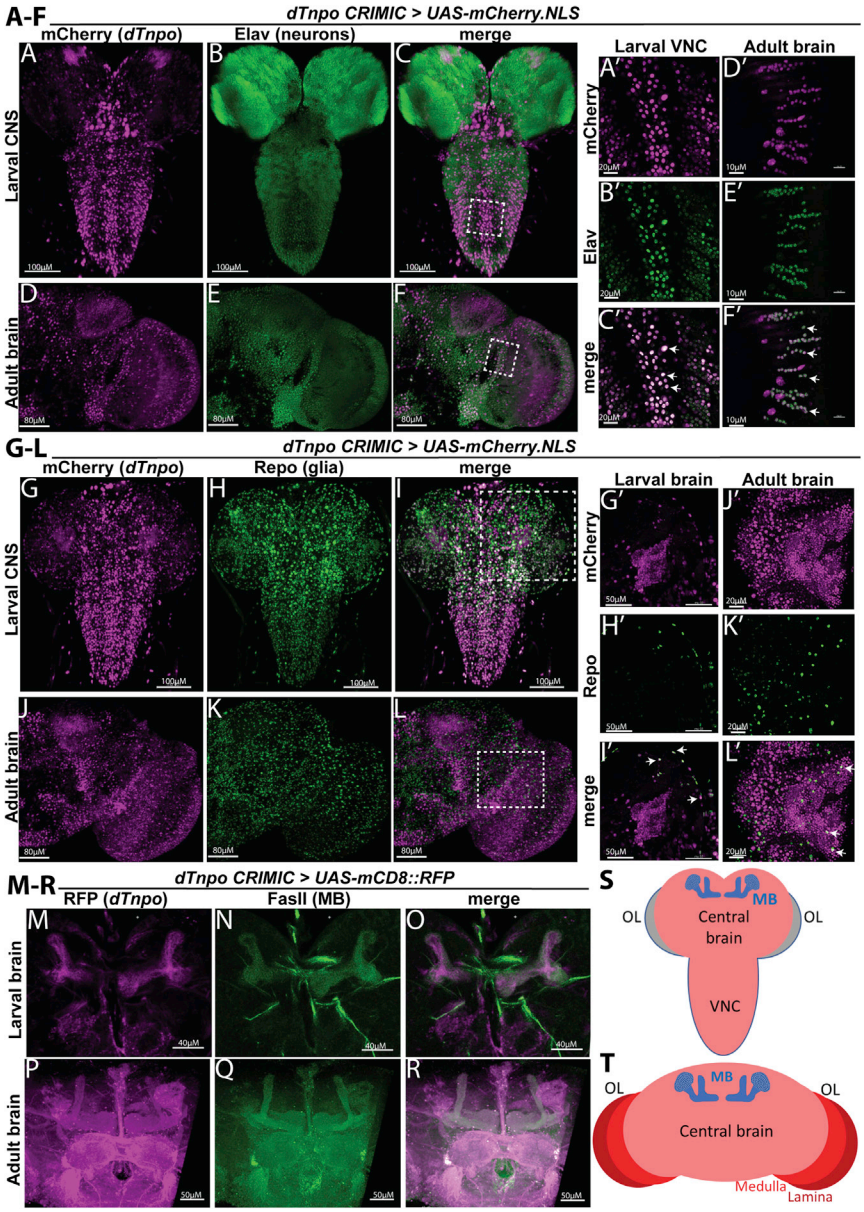

Figure 3. *dTnpo* is highly expressed in neurons, including mushroom body neurons

The *dTnpo CRIMIC* (*T2A-GAL4*) allele was used to drive expression of *UAS-fluorescent reporter transgenes*.

(A–L) *UAS-mCherry.NLS* (nuclear mCherry) was expressed and tissue were dissected from L3 larvae (CNS, includes central brain and VNC) or adults (brain). Shown is half of the adult brain. Tissue were counterstained with markers for neurons (Elav) or glia (Repo). Z stacked images showing *dTnpo* expression pattern compared to neurons (A–F) or glia (G–L). Dashed squares indicate regions used in (A′)–(L′).

(A′–L′) Single slice images were used to better visualize cellular co-localization of mCherry.NLS signal with neurons or glia. White arrows highlight co-localized nuclei with most neurons and some glia.

(M–R) *dTnpo CRIMIC* driven expression of *UAS-mCD8::RFP* (membrane-bound RFP) and FasII counter-staining confirmed overlap of *dTnpo* expression and mushroom body (MB) neurons in both larval and adult brains.

(S and T) Schematics of the larval CNS (S) and adult brain (T) highlighting MB neurons (blue), the ventral nerve cord (VNC), the central brain, and optic lobes (OL). The adult OL includes the medulla and lamina. The adult brain also includes the subesophageal ganglion (not shown in the schematic).

images, there is no obvious overlap with glia and cells expressing mCherry (*dTnpo*) in larvae (Figures 3H and 3I) and adults (Figures 3K and 3L). However, in single-slice images of larval CNS (Figures 3G′–3I′) and adult brains (Figures 3J′–3L′), some Repo-positive cells show overlap with mCherry-positive cells, arguing that a small subset of glia express *dTnpo*.

The MB is of interest as this is the primary learning and memory center in *Drosophila*[74] and the individuals in our cohort present with intellectual disability. To confirm *dTnpo* expression in these cells, *UAS-mCD8::RFP* (RFP fluorescent protein localized to the membrane) was expressed using the *dTnpo CRIMIC* allele and tissue were counterstained with an established MB marker, FasII,[75] in larvae (Figures 3M–3O) and adults (Figures 3P–3R). Indeed, we see consistent overlap between RFP (*dTnpo*) and FasII signal, supporting that *dTnpo* is expressed in these neurons.

In sum, we found that *dTnpo* is highly expressed in a subset of neurons, including those that mediate associative learning, in the larval CNS and adult fly brain.

dTnpo is required for neuron function and maintenance

We next examined whether *dTnpo* was essential in fly neurons. We first assessed whether *dTnpo* was required during neural development. When we express *UAS-dTnpo RNAi-1* in neuroblasts (neural stem cells) using *insc-GAL4*, no significant reductions in L3 larval CNS size are seen (Figure S2). In contrast, expressing *UAS-dTnpo RNAi-1* using the pan-neuronal driver, *elav-GAL4*, is lethal (Figure S1F).

To avoid developmental lethality caused by expressing *UAS-dTnpo RNAi-1* with *elav-GAL4*, we utilized a drug, RU486, inducible version of this neuronal driver, *elav-GAL4[GeneSwitch]* (*elav-GAL4^{GS}*)[76] to express the *dTnpo* RNAi-1. 1- to 2-day-old flies were transferred onto RU486-containing food, thus avoiding RNAi expression prior to adulthood. These animals were maintained on RU486 and survival curves were calculated for animals expressing *UAS-dTnpo RNAi-1* compared to animals expressing *UAS-control (Luciferase) RNAi*. Interestingly, there is a significant decrease in survival when *dTnpo* is downregulated using

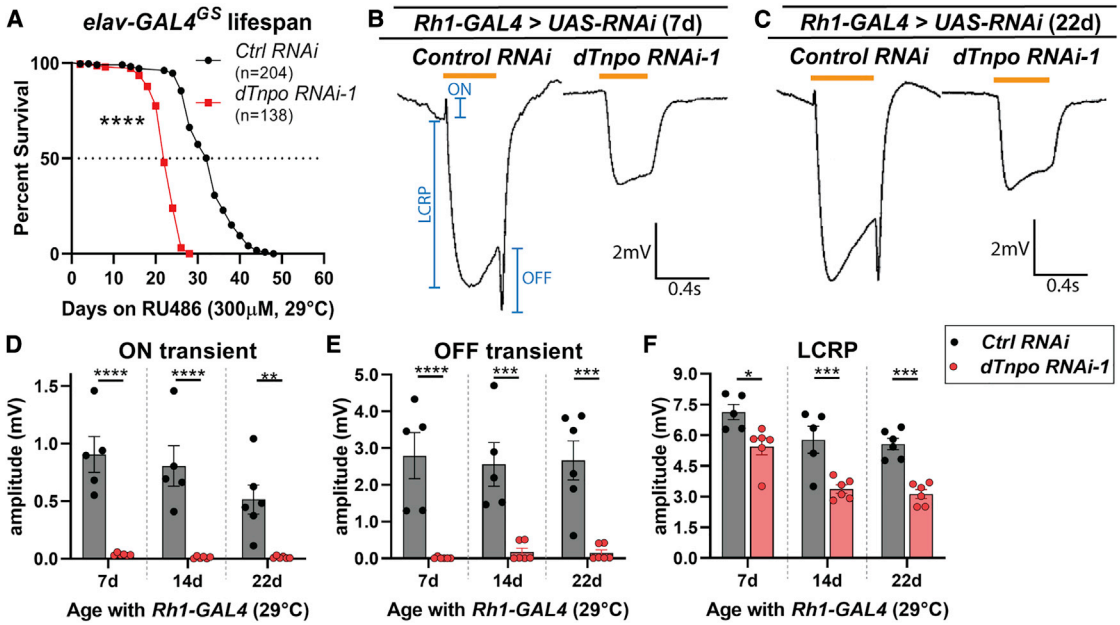

Figure 4. Fly *Transportin* is required in neurons for survival and eye function

(A) The drug-inducible *elav-GAL4*^{GS} driver was used to express RNAi in adult fly neurons while avoiding RNAi expression during development. Expression of *dTnpo* RNAi-1 significantly impacts animal survival, indicating a progressive loss of neuron function due to *dTnpo* loss.

(B and C) *Rh1-GAL4* was used to express RNAi in mature photoreceptor neurons and electroretinograms (ERGs) were used to measure neuronal function at 7 days, 14 days, and 22 days. Blue annotation shows where amplitudes are measured. Orange bars indicate the light pulses.

(D–F) *dTnpo* RNAi-1 nearly abolishes ON and OFF transients (D, E) and reduces the light coincident receptor potential (LCRP; F) compared to a control RNAi.

Statistics: (A) log-rank, (D–F) 2-way ANOVAs with Sidak's multiple comparisons test. *$p < 0.02$, **$p < 0.01$, ***$p < 0.001$, ****$p < 0.0001$. Each dot represents the mean of 5 recorded ERGs per animal. The mean from 5–6 animals is shown. Error bars denote SEM; "Control (Ctrl) RNAi" is *UAS-Luciferase RNAi* (TRiP.JF01355). *UAS-dTnpo RNAi-1* is TRiP.HMJ23009.

RNAi expression in the adult fly neurons (Figure 4A). 50% of *UAS-dTnpo RNAi-1*-expressing animals die by 22 days compared to 32 days for *control RNAi*-expressing animals. The max survival is also decreased by 20 days with 100% of *dTnpo RNAi-1* animals dying by 28 days, compared to 48 days for *control RNAi* animals.

To examine whether *dTnpo* is required for neuronal activity, we performed electroretinograms (ERGs) on *UAS-dTnpo RNAi-1* and *UAS-control RNAi*-expressing animals (Figures 4B–4F). ERGs are an established method for measuring neuron dysfunction in the synaptic circuit that makes up the fly optic system. ERGs quantify the light coincident receptor potentials (LCRP) and ON/OFF transients in the adult eye.[77–79] LCRP amplitudes measure the phototransduction pathway that is dependent on light exposure.[77,78] ON/OFF transients measure synaptic transmission between photoreceptor neurons and post-synaptic neurons in the lamina.[77,78] At 7 days, the downregulation of *dTnpo* by expressing RNAi in mature photoreceptor neurons using *Rh1-GAL4* causes significant changes to the ON and OFF transient amplitudes (Figures 4D and 4E), indicating a loss of synaptic activity. LCRP defects are also observed in *dTnpo* RNAi-1-expressing animals based on reductions in depolarization amplitude (Figure 4F). This impact seems to become stronger with age as there is a reduction of 24% in LCRP at 7 days when compared to control RNAi-expressing flies. This reduction is more robust by 14 days and 22 days at 42% and 44%, respectively.

In sum, *dTnpo* expression in neurons was found to be essential for animal survival. Further, neuronal function in the fly eye is disrupted by *dTnpo* loss, supporting that *dTnpo* is required in mature neurons.

Upregulation of *dTnpo* causes similar phenotypes to *dTnpo* LoF mutants

Thus far, we found that phenotypes associated with *dTnpo* loss are dosage dependent. We therefore considered whether *dTnpo* overexpression could also be detrimental. We obtained a fly line, *UAS::dTnpo*^{GS11030}, that contains a P-element insertion with a *UAS* element upstream of the *dTnpo* gene.[80] This allows us to upregulate *dTnpo* under control of the *GAL4/UAS* system[69] by a 25- ± 8.1-fold increase in *dTnpo* mRNA levels (Figure 5A). Interestingly, upregulation of *dTnpo* using the ubiquitous driver, *da-GAL4,* causes lethality after pupariation (Figure 5B). Further, upregulation of *dTnpo* in both early (*ey-GAL4*) and late (*GMR-GAL4*) eye development causes rough eye phenotypes and reduced eye size (Figures 5B and 5C). *dTnpo* upregulation in the wing using *nub-GAL4* causes wing notching and

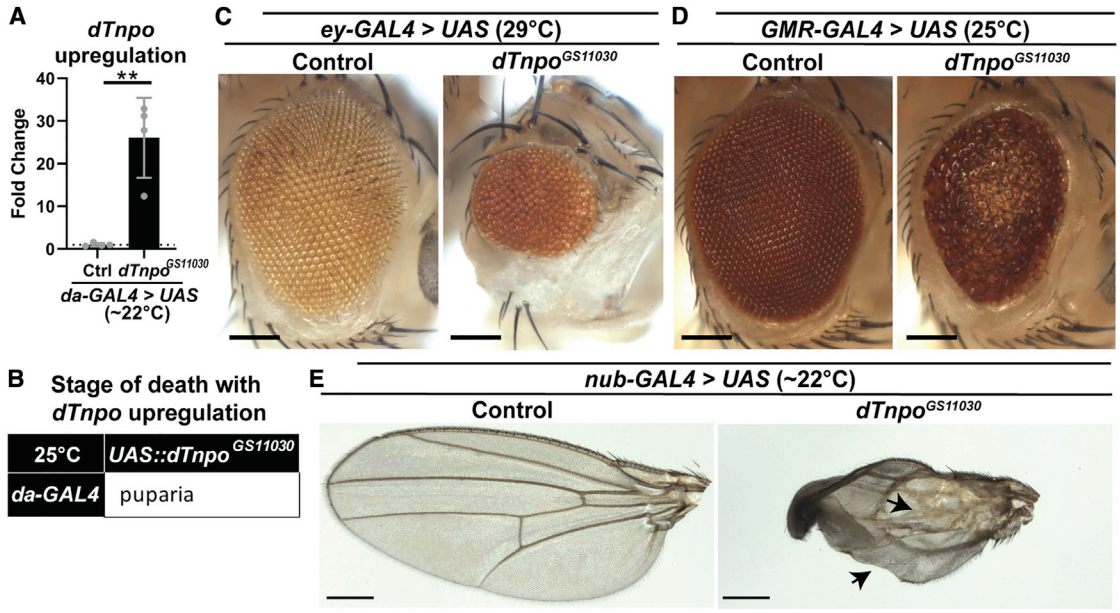

Figure 5. Upregulation of *dTnpo* disrupts morphology of eyes and wings
(A) Ubiquitous expression of *UAS::dTnpo*^{GS11030} using *da-GAL4* in flies causes a 25-fold increase in *dTnpo* mRNA levels by qPCR. L3 larvae were analyzed at 22°C. Unpaired t test, ***p = 0.0003. Each dot represents the mean from replicate wells per sample. The mean from 4 individual samples is shown. Error bars denote SD.
(B) *da-GAL4>UAS::dTnpo*^{GS11030} animals do not survive beyond pupariation at 25°C.
(C and D) Upregulation of *dTnpo* during eye development, using either *ey-GAL4* (early development) or *GMR-GAL4* (late development) driven expression of *UAS::dTnpo*^{GS11030}, causes small eyes and rough eye phenotypes. Scale bar = 100 μm.
(E) *nub-GAL4* driven expression of *UAS::dTnpo*^{GS11030} causes notch and blister phenotypes (arrows) in the fly wing. Scale bar = 200 μm. "Control (Ctrl)" is *UAS-empty*.

large blisters in 100% of animals (Figure 5D). In sum, we see that upregulating *dTnpo* causes similar phenotypes as *dTnpo* loss (see Figures 2 and S1).

Ectopic expression of human *TNPO2* in flies causes developmental toxicity

We next aimed to define whether proband-associated variants in *hTNPO2* could alter the function of the encoded protein *in vivo*. For this purpose, we established a series of *UAS-hTNPO2* fly lines expressing wild-type (WT; reference) or variant human *TNPO2* cDNA (GenBank: NM_0011 36196.1) under control of the *GAL4/UAS* system. We selected 6 of the 14 variants that are at conserved amino acids for analysis, two from each protein domain. This included p.Gln28Arg, p.Asp156Asn, p.Trp370Arg, p.Trp 370Cys, p.Ala546Val, and p.Trp727Cys. We confirmed that these lines properly express the *UAS-hTNPO2* transgenes at comparable levels using western immunoblots and an antibody specific to human TNPO1/2 (Figure 6A). We expressed *UAS* transgenes in 1- to 2-day-old adult animals using the drug-inducible, ubiquitous driver, *da-GAL4*^{GS}, to avoid any toxicity during development.

Previously, we had found that animals trans-heterozygous for the hypomorph alleles, *dTnpo*^{Gly736Asp} and *dTnpo CRIMIC*, did not survive past larval stage 3 (see Figure 2C). Thus, we examined whether expression of *hTNPO2* could rescue this phenotype. Using the *dTnpo CRIMIC (T2A-GAL4)* allele, we expressed *UAS-hTNPO2:WT*^{HA} (wild-type *hTNPO2* cDNA with a 3′ 3xHA-tag) or control *UAS-(empty)* in these *dTnpo* trans-heterozygous hypomorph animals. No rescue is observed with the expression of *hTNPO2* cDNA in these mutant animals (Figure S3A). We noted that *hTNPO2:WT* expression causes death earlier, at L2, rather than L3 when compared to *UAS-(empty)* control expressing flies, demonstrating that the expression of *hTNPO2:WT* increased, rather than reduced, toxicity in these *dTnpo* mutant flies. We also tested whether five of the variants found in our cohort could rescue lethality in *dTnpo* trans-heterozygous animals. Interestingly, the *p.Trp370Cys* and *p.Ala546Val* variants result in death at L3 rather than L2 when compared to *hTNPO2:WT*. The other variants tested—*p.Gln28Arg*, *p.Asp156Asn*, and *p.Trp727Cys*—caused lethality at L2 like *hTNPO2:WT*.

We next considered if the lack of rescue seen with expression of *hTNPO2* in *dTnpo* trans-heterozygous hypomorph animals is due to the overexpression of *hTNPO2* in flies being toxic. This is because we found that robust upregulation of *dTnpo* was toxic (see Figure 5) and the expression of *UAS-hTNPO2* by the *dTnpo CRIMIC* allele will result in an overexpression of *hTNPO2*,[42] albeit likely at significantly lower levels than that caused by the *UAS::dTnpo*^{GS11030} allele.[69] Thus, we would have two sources of toxicity in rescue experiments, that from the mutations in *dTnpo* and that from overexpressing *hTNPO2*. To test this hypothesis, Mendelian ratios were calculated for progeny from crosses between *da-GAL4* and *UAS* fly lines, including *UAS-hTNPO2* lines and the control *UAS-(empty)*

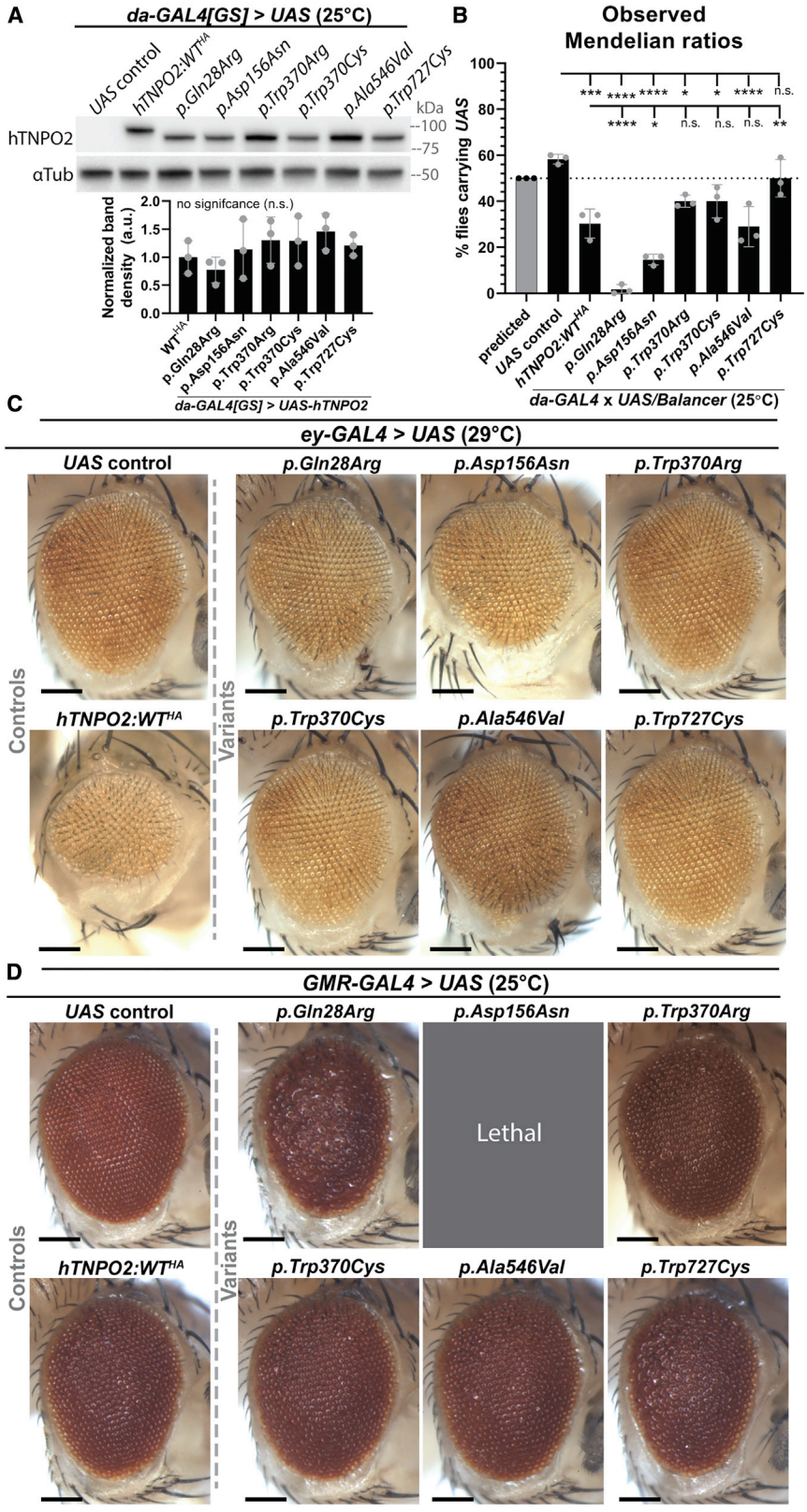

Figure 6. Variants in *hTNPO2* cause different amounts of toxicity compared to wild-type *hTNPO2* during fly development and in the eye

(A) *UAS-hTNPO2* fly lines were generated. Western immunoblots (WBs) confirmed hTNPO2 protein levels are similar between lines using a drug-inducible ubiquitous driver (*da-GAL4*^{GS}) to express transgenes and a human TNPO1/2 antibody. Normalized hTNPO2 band density from three independent westerns were quantified. Each dot represents one independent sample. The mean from 3 individual samples is shown.

(B) *da-GAL4* driven ectopic expression of *UAS-hTNPO2:WT*^{HA} reduces Mendelian ratios compared to *UAS* control flies, demonstrating toxicity during development. Variants *p.Gln28Arg* and *p.Asp156Asn* are more toxic than *hTNPO2:WT* whereas *p.Trp727Cys* is less toxic. Each dot represents one independent cross with >100 animals scored. The mean from three independent crosses is shown.

(C and D) Ectopic expression of *UAS-hTNPO2:WT*^{HA} disrupts eye development using either *ey-GAL4* (early development) or *GMR-GAL4* (late development). Scale bars = 100 μm.

(C) With *ey-GAL4>hTNPO2:WT*^{HA}, eyes are smaller than controls and have a rough eye phenotype. *p.Trp370Cys* and *p.Trp370Arg* are less toxic.

(D) With *GMR-GAL4>hTNPO2:WT*^{HA}, eyes are moderately smaller and there is a mild rough eye phenotype compared to controls. *p.Gln28Arg* and *p.Asp156Asn* are more toxic.

Statistics: 1-way ANOVAs with Dunnett's (A) or Tukey's (B) multiple comparisons test. no significance (n.s.) ≥ 0.05, *p < 0.05, **p < 0.01, ***p < 0.001, ****p < 0.0001. Error bars denote SD "UAS Control" is *UAS-(empty)*.

line (Figure 6B). As expected, 58% ± 2.1% of control progeny carry the *UAS* transgene. In contrast, only 28% ± 6.4% of progeny from *UAS-hTNPO2:WT*^{HA} crosses carry the *UAS* transgene, showing that significant toxicity occurs during development (Figure 6B). The presence of the HA-tag on the *hTNPO2:WT* transgene does not alter this effect (Figure S3B). Overall, these data demonstrate that ubiquitous, ectopic expression of *hTNPO2* is toxic.

We also investigated whether proband-associated variants could induce the same toxicity as wild-type *hTNPO2*. Notably, *p.Gln28Arg* and *p.Asp156Asn* are more toxic than *hTNPO2:WT* (Figure 6B). Further, variants *p.Trp370Arg*, *p.Trp370Cys*, and *p.Ala546Val* cause similar toxicity compared to that caused by *hTNPO2:WT* expression (Figure 6B). In contrast, the *p.Trp727Cys* variant is significantly less toxic than *hTNPO2:WT*, producing 50% ± 8.2% of *UAS* carrying progeny (Figure 6B).

In summary, ectopic expression of *hTNPO2* in flies causes toxicity consistent with phenotypes observed

when upregulating *dTnpo* (see Figure 5). As three of six proband-associated variants tested caused significant differences in the amount of toxicity than that caused by wild-type *hTNPO2*, these data suggest that these variants alter the function of the hTNPO2 protein. Specifically, p.Gln28Arg and p.Asp156Asn may cause gain-of-function (GoF) effects and p.Trp727Cys may cause LoF effects.

Toxicity caused by variants in the fly eye differ from that of wild-type *hTNPO2*

Next, we assessed whether ectopically expressing wild-type and variant *hTNPO2* in the fly eye can cause morphologic disruptions similar to wild-type *dTnpo* upregulation (see Figure 5). Using *ey-GAL4*, expression of *hTNPO2:WT* causes a smaller eye and a rough eye phenotype compared to animals expressing a *UAS* control (Figure 6C). Expression of the *p.Trp727Cys* variant leads to eyes more similar to controls than *hTNPO2:WT* (Figure 6C), consistent with it being less toxic than *hTNPO2:WT* during animal development (see Figure 6B). Interestingly, variants *p.Trp370Arg* and *p.Trp370Cys* are also less toxic than *hTNPO2:WT*, suggesting that during early eye development these variants act as LoF-variants. Expression of variants *p.Gln28Arg*, *p.Asp156Asn*, and *p.Ala546Val* cause similar eye phenotypes as *hTNPO2:WT*.

To further explore the impacts of variants at later stages of the developing eye than those affected by *ey-GAL4*, we expressed *UAS* transgenes using *GMR-GAL4*. Ectopic expression of *hTNPO2:WT* causes a moderate rough-eye phenotype and smaller eyes compared to animals expressing *UAS* control (Figure 6D). Consistent with previous data using *da-GAL4* (see Figure 6B), expression of *p.Gln28Arg* and *p.Asp156Asn* cause more toxicity than *hTNPO2:WT* expression (Figure 6D). Specifically, *p.Gln28Arg* causes a more robust rough eye phenotype and smaller eyes and *p.Asp156Asn* causes developmental lethality. *GMR-GAL4* is expressed at low levels in the larval brain[81,82] and has been reported to cause lethality in extremely toxic situations.[44,83] In contrast, eye phenotypes caused by expression of *p.Trp370Arg*, *p.Trp370Cys*, and *p.Ala546Val* are similar to *hTNPO2:WT* (Figure 6D). In turn, expressing *p.Trp727Cys* causes a slightly more robust rough eye phenotype compared to *hTNPO2:WT* expressing animals.

In sum, ectopic expression of wild-type *hTNPO2* in the fly eye causes morphologic defects. Interestingly, these defects are different when comparing animals expressing proband-associated variants versus *hTNPO2:WT*. The specific effects of each variant are dependent on the developmental stage during which the transgenes are expressed in the fly eye, fitting with *TNPO2* encoding a pleiotropic protein that may play different roles at different stages of development.

Toxicity caused by variants in the developing wing differ from that of wild-type *hTNPO2*

Thus far, we defined differences between toxicity induced by ectopically expressing wild-type and variant *hTNPO2* by expressing them ubiquitously during development or in the developing fly eye (see Figure 6). Given that toxicity in response to expressing these proteins may differ depending on the tissue, we further analyzed impacts in the fly wing using *nub-GAL4*. When *UAS-hTNPO2:WT^{HA}* was ectopically expressed in the developing wing, progeny had blister phenotypes and gain-of-vein phenotypes and the wings were smaller than control *UAS* wings (Figure 7A). *hTNPO2:WT* phenotypes are 50% ± 8.5% penetrant, allowing us to quantitatively analyze the effects of proband-associated variants in this tissue (Figure 7B). Consistent with previous data, expression of *p.Gln28Arg* and *p.Asp156Asn* cause more severe wing phenotypes than *hTNPO2:WT* expressing animals (Figure 7A). In addition to blisters and gain-of-vein phenotypes, wings from *p.Gln28Arg* and, particularly, *p.Asp156Asn*, commonly have notch phenotypes, are smaller, and have more disruptions to wing inflation than *hTNPO2:WT* animals. Further, blister and notch phenotypes are significantly more penetrant with these variants, at 99.6% ± 0.2% and 98.8% ± 0.5%, respectively (Figure 7B). In contrast, animals expressing variants *p.Trp370Arg*, *p.Trp370Cys*, and *p.Ala546Val* rarely have blister phenotypes (Figure 7A) with a concomitant and significant reduction in phenotype penetrance compared to *hTNPO2:WT* expressing animals (Figure 7B). Interestingly, animals expressing *p.Ala546Val*, which had minimal effects in the developing animal and eye (see Figure 6), showed few defects and phenotype penetrance was significantly lower than that for *hTNPO2:WT* expressing animals at 0.8% ± 0.5%. Last, expression of *p.Trp727Cys*, which had variable effects in other tissues, causes a more severe gain-of-vein phenotype compared to *hTNPO2:WT* expressing animals (Figure 7A). However, penetrance of the blister and notch phenotypes is similar between animals expressing *p.Trp727Cys* and *hTNPO2:WT* (Figure 7B).

In sum, ectopic expression of *hTNPO2* in the developing fly wing causes morphologic defects that are altered by proband-associated variants. Concomitantly, phenotype penetrance is significantly different for most variants.

Discussion

We identified 15 individuals who carry pathogenic coding variants in the pleiotropic protein, TNPO2. Probands uniformly present with global developmental delay (GDD), including speech/motor deficits and intellectual disability. The majority also have behavioral deficits, feeding difficulties, dysmorphic features, strabismus, and muscle tone abnormalities (primarily hypotonia). Movement and neurological disorders (e.g., tremors, ataxia) and neurological features, including seizures and abnormal MRIs, are also seen. Using *Drosophila*, we found that *Transportin* (*dTnpo*) is an essential gene during animal development and is required for proper eye and wing formation. Malformations caused by decreasing *dTnpo* activity are dosage dependent with greater reductions in *dTnpo* activity causing more severe

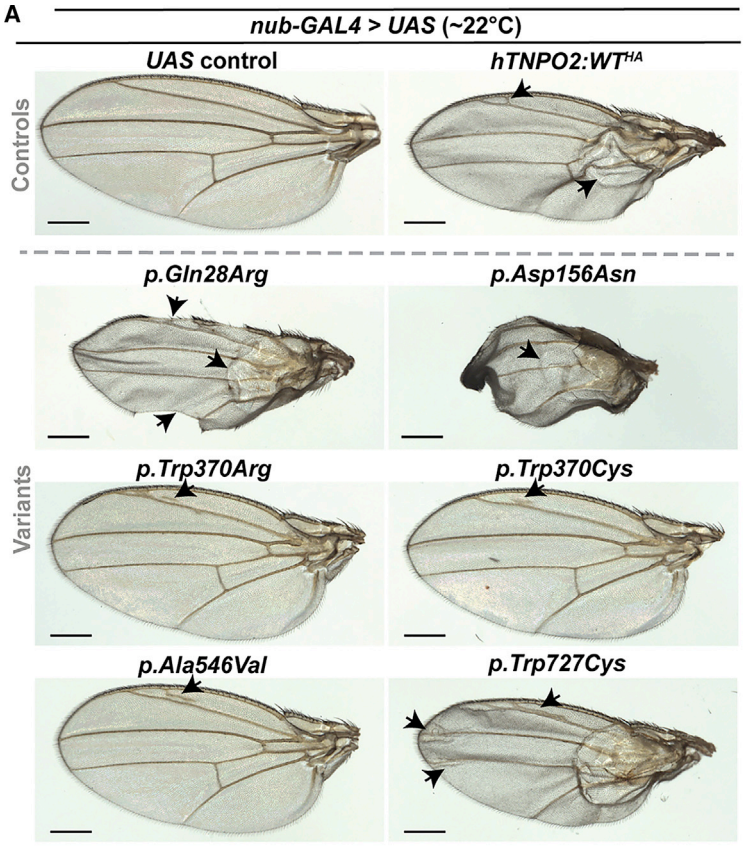

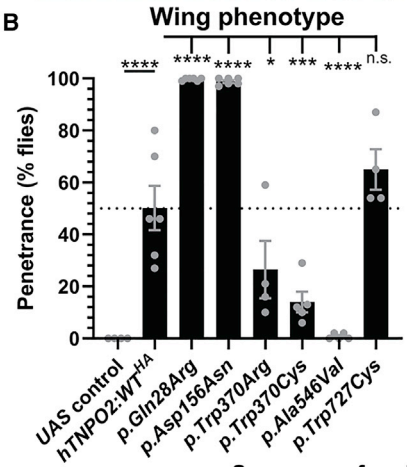

C

Summary of variant-induced toxicity in comparison to wild-type *hTNPO2*-induced toxicity

	Patient-associated variant					
	p.Gln28Arg	p.Asp156Asn	p.Trp370Arg	p.Trp370Cys	p.Ala546Val	p.Trp727Cys
Total impact	↑↑↑	↑↑↑	↓↓	↓↓	↓	↓↓↑
Domain	RAN binding		Acidic loop		Cargo binding	
Ubiquitous expression						
da-GAL4	↑↑↑	↑↑	–	–	–	↓↓
Expression in the developing eye						
ey-GAL4 (early)	–	–	↓↓	↓↓	–	↓
GMR-GAL4 (late)	↑↑	↑↑↑	–	–	–	↑
Expression in the developing wing						
nub-GAL4	↑↑↑	↑↑↑	↓↓	↓↓	↓↓↓	↑

Figure 7. Variants alter *hTNPO2*-induced phenotypes and penetrance in the fly wing and impact of the variants corresponds with their location within the protein

(A) Ectopic expression of *UAS-hTNPO2:WT*^{HA} using *nub-GAL4* disrupts wing development, causing notching, blisters, and gain-of-vein phenotypes (arrows). *p.Trp370Cys*, *p.Trp370Arg*, and *p.Ala546Val* have less severe phenotypes whereas *p.Gln28Arg* and *p.Asp156Asn* are significantly more toxic. *p.Trp727Cys* has a moderately stronger gain-of-vein phenotype than *hTNPO2:WT*. Scale bar = 200 μm.

(B) Blister and notch phenotypes caused by *hTNPO2* expression in the wing occurs in 50% of wings, representing penetrance. Penetrance is significantly different for all variants except *p.Trp727Cys*. Statistics: 1-way ANOVAs with Dunnett's multiple comparisons test. No significance (n.s.) ≥ 0.05, *p < 0.05, ***p < 0.001, ****p < 0.0001. Error bars denote SEM. Each dot represents the results from one cross with >50 animals scored. The mean from two independent experiments that included 2–3 individual crosses is shown.

(A and B) "*UAS Control*" is *UAS-(empty)*.

(C) Table summarizing phenotype severity associated with variants when compared to *hTNPO2:WT*-associated phenotypes. Symbols: strong decrease in toxicity (green arrows), strong increase in toxicity (red arrows), mild increase in toxicity (orange arrows), no obvious difference in toxicity (dash). *p.Trp727Cys* strongly reduces toxicity in two situations and mildly increases toxicity in two situations, earning two green and one red arrow in the summary.

defects. Interestingly, upregulation of *dTnpo* causes similar defects as *dTnpo* loss. We further found that *dTnpo* is required in the fly nervous system. It is expressed mostly in neurons and abundant in mushroom body (MB) neurons. Downregulating *dTnpo* in mature neurons disrupts their function and reduces animal survival. Ectopic expression of wild-type, human *TNPO2* causes similar phenotypes in the fly as gain and loss of *dTnpo*, suggesting that its function is evolutionarily conserved. Interestingly, ectopic expression of *UAS-hTNPO2* transgenes carrying proband-associated variants cause different levels of toxicity compared to animals expressing wild-type *UAS-hTNPO2*, supporting that these variants disrupt the encoded protein's normal activity *in vivo*. Impacts seem to vary based on the variant's location within the protein (discussed below). In conclusion, these data demonstrate that *de novo* coding variants within *TNPO2* can alter the function of the encoded, essential protein

and are associated with developmental phenotypes in individuals.

Potential roles of *TNPO2* variants in disease

While *de novo* variants in *TNPO2* had been recorded in individuals with intellectual disability, previous studies did not find that *TNPO2* variants were a significant cause of GDD in large datasets that included hundreds to thousands of cases.[84–87] Our independent identification of 15 individuals with GDD that carry pathogenic *TNPO2* variants and functional studies using *Drosophila* provide strong evidence of the important role this gene plays in human development and in the nervous system. Together, these data demonstrate that while *TNPO2* variants are associated with GDD, this is a rare cause of disabilities.

Our fly data demonstrate that all variants tested can alter the anticipated function of *hTNPO2 in vivo* (see Figures 6 and 7). These data suggest that the impact of a variant depends on its position within the protein in addition to the tissue and developmental stage during which the transgenes are expressed. To better understand how these variants compare to wild-type *TNPO2*, we compiled a summary of our fly data that used ectopic expression of *TNPO2* cDNA (Figure 7C; extended data in Figure S3C). Interestingly, expression of variants that fall within the RAN binding domain were significantly more toxic than *hTNPO2:WT* in almost all conditions. These data suggest these are GoF variants. In contrast, expression of variants that fall within the acidic loop of the protein tended to be less toxic than *hTNPO2:WT* expression, suggesting they are LoF variants. As these two variants fall at the same amino acid in the protein, future studies are needed to test additional variants from within this domain. Interestingly, we also observed that expression of variants in the cargo binding domain of hTNPO2 have more variable effects when compared to *hTNPO2:WT* expression. Generally, these have reduced toxicity compared to wild-type *hTNPO2*, but the tissue assayed seems more critical in defining their impact. This fits with the known function of this domain as cargoes are likely to differ between tissues and ages. Specifically, in our fly data *UAS-hTNPO2:p.Ala546Val* (associated with proband 11) has similar toxicity when ubiquitously expressed and when expressed in the fly eye as compared to *UAS-hTNPO2:WT*. However, expression of this variant is significantly less toxic than *hTNPO2:WT* in the fly wing. Consistent with these data, proband 11 shows fewer phenotypes than other persons within our cohort (see Table 1, Data S1, and Figure 1). Thus, this variant may be tissue specific. In addition to *p.Ala546Val*, the current fly data argue that the impact of *p.Trp727Cys* is also tissue dependent. Specifically, expression of this variant is significantly less toxic than wild-type *TNPO2* with *da-GAL4* (ubiquitous) and *ey-GAL4* (early eye formation) and only mildly more toxic than wild-type *TNPO2* with *GMR-GAL4* (late eye formation) and *nub-GAL4* (wing formation). In sum, these data suggest that it is more of a LoF variant than a GoF variant while mechanistic studies are needed in each tissue to strengthen these results. Interestingly, disease presentation in proband 15 (carries *p.Trp727Cys*) seems to diverge from the majority of the cohort as this individual presents with hypertonia and no signs of hypotonia, is the only individual with notable sleep deficits, and is the only individual with a rigid gait. Also, this person does not have any known neurological features despite undergoing an EEG and MRI testing. Overall, more directed investigation is needed to better understand the different roles of these cargo binding domain variants while considering their impacts in different tissues and at different developmental stages.

Interestingly, the *p.Lys152del* variant in proband 5 is only found at a 16% mosaicism by Sanger sequencing (21% by WGS) in blood. We believe that the deletion of p.Lys152 within this critical domain can explain this individual's features given similarities of this person's symptoms to others in the cohort, our fly data showing that the nearby variant of *p.Asp156Asn* significantly impacted the function of *TNPO2* in multiple tissues (see Figure 7C), and the fact that this variant is at a conserved amino acid in multiple organisms, including mice (see data in MARRVEL[48]). It is also important to note that the amount of mosaicism in other tissues is not known.

Except for *p.Ala546Val* (proband 11), and potentially *p.Trp727Cys* (proband 15), no obvious association with the other variants tested in the fly and symptoms or severity of individual's features are observed. We hypothesize that this is due to the findings that both up- or downregulation of *Transportin* in the fly cause similar phenotypes (see Figures 2, 5, and S1). It is likely that loss of *dTnpo* disrupts the shuttling of cargoes into the nucleus and this disrupts multiple pathways important during development and for neuron maintenance (see below). Speculatively, we predict that upregulation of *dTnpo* and ectopic expression of *hTNPO2* causes similar phenotypes as *dTnpo* loss as these would cause an accumulation of the Transportin protein intracellularly. This could sequester the dTnpo cargos, making them unavailable to perform their normal functions. Thus, gain-of-function-associated toxicity would still result in similar phenotypes as loss-of-function mechanisms.

It is important to note that TNPO1/2 function in many pathways including ciliogenesis, mitotic spindle assembly, and nuclear envelope assembly. Further, it was recently shown that when TNPO1 binds the nuclear pore complex RAN GTP was retained in the nucleus.[88] Thus, disrupting the function of TNPO2 could not only impact its cargoes but also the RAN GDP/GTP gradient used to drive the activity of this and other proteins.[7] Notably, due to this pleiotropic nature of TNPO2, the impact of up/downregulating the fly gene, the impact of ectopically expressing the human gene in the fly, and the impact of variants on the endogenous function of the protein encoded by human *TNPO2* in individuals is likely to be very complex. Interestingly, phenotypic variability of monogenic causes of neurologic disorders has been described for other genetic

conditions, such as those associated with *EEF1A2* (MIM: 602959).[89] Overall, our fly data demonstrate that Transportin's activity would likely need to be tightly regulated to prevent disease.

Supporting the hypothesis that both gain- or loss-of-function variants can contribute to *TNPO2*-associated disorder, it is notable that copy number variants (CNVs) that include *TNPO2*, both deletions and duplications, have both been reported as pathogenic in ClinVar[90] by studies that evaluated CNVs in individuals with developmental delays, including accession numbers: VCV000059111.1 (SCV000080263.4; duplication)[91] and VCV000153069.1 (SCV000182485.3; deletion).[92] While the region of these CNVs includes other genes, it is intriguing to consider that the dosage sensitivity of *TNPO2* could contribute to developmental phenotypes in these individuals. In particular, the whole gene deletion of *TNPO2* in these cases are consistent with a potential haploinsufficiency as a part of the disease mechanism(s) associated with this gene.

In sum, our fly data support that any disruptions to *TNPO2* activity (gain or loss) in individuals is likely to cause similar symptoms. Further, coding variants in *TNPO2* can alter the function of the protein with ectopic expression of transgenes. Future mechanistic studies should focus on differences between the variants, considering the impact of variants as gain-of-function, loss-of-function, or dominant-negative mutations in multiple contexts and tissues. Further, additional variants will need to be tested to better understand the potential association between protein domain and a variant's impact on *TNPO2*'s function. Last, as our studies depended on ectopic expression of human *TNPO2*, future studies should focus on defining the mechanisms underlying the impact of individual variants in an endogenous system.

TNPO2 during development

Consistent with TNPO2 being a pleiotropic protein, this gene is required in multiple tissues in the fly (see Figures 2, 4, and S1). Impacts of losing *Transportin* during development are dosage dependent with stronger *dTnpo* mutants and *dTnpo*-targeting RNAi causing more severe defects (see Figures 2 and S1). Upregulation of *dTnpo* and ectopic expression of its human ortholog, *hTNPO2*, causes similar defects (see Figures 5, 6, and 7), potentially by titering cargoes away from their normal function(s) as discussed above. We note that our *dTnpo* mutant and RNAi studies rely on robust depletion of *dTnpo*, either through the use of homozygous mutant animals or the significant downregulation of *dTnpo* mRNA, respectively (see Figures 2 and S1). Further, the *UAS::dTnpo*^{GS11030} allele causes a dramatic upregulation of the fly gene. Future studies should titer the expression of *dTnpo* to see when phenotypes occur and consider the possibility that heterozygous mutant animals may have minor anomalies. It is also important to note that the ectopic expression of the *UAS-hTNPO2* lines is not expected to cause such robust overexpression of the Transportin protein as was seen with the *UAS::dTnpo*^{GS11030} allele.[69] However, further investigations into the impacts of the variants in a system that does not rely on ectopic expression of genes would likely reveal additional information as to the role these variants play in disease.

Interestingly, TNPO1/2 interact with multiple, conserved factors important in developmental pathways, including NF-κB signaling,[18] hedgehog signaling,[60] insulin signaling,[29] and Ras/ERK signaling.[17,93,94] These pathways are involved in multiple aspects of fly eye and wing formation and disruptions can cause similar phenotypes to what we observe in our studies.[65,67,68] Thus, data support that *TNPO2* coding variants could impact multiple developmental pathways simultaneously and this could explain the varied features observed in our cohort (see Data S1). Further, *TNPO2* was found to be critical for HuR/ElavL1-mediated muscle cell differentiation in cultured murine myoblasts.[11] This may be related to muscle tone abnormalities in our cohort (see Table 1). Last, it is notable that most of the *TNPO2* cohort present with gastrointestinal abnormalities while multiple TNPO1/2 cargoes are involved in stress pathways associated with chronic intestinal inflammation in mammals, including components of the Activator Protein-1 (AP1) transcription complex,[95–98] NEMO,[18,99] ADAR1 (MIM: 146920),[100,101] and HSP70 (MIM: 140550).[16,102] While gastrointestinal abnormalities are commonly associated with GDD, symptoms may be exacerbated by *TNPO2* variants. Overall, our findings in *Drosophila* support that *hTNPO2* is an important developmental gene that can impact multiple systems.

TNPO2 in the nervous system

Accumulating data show that *TNPO2* is an important neuronal gene. We found that *dTnpo* is primarily expressed in a subset of neurons, including MB neurons, in the fly CNS (see Figure 3). These findings are consistent with mammalian data as *TNPO1/2* is highly expressed in the brain.[9,10,53] In mouse brains, *Tnpo2* seems to be more highly expressed overall than *Tnpo1*[9,10] but this may depend on the brain region.[53] Interestingly, when considering regions associated with memory, *Tnpo2* was shown to be more highly expressed in the cerebral cortex than *Tnpo1* and both genes were highly expressed in the hippocampus and cerebellum.[53] The hippocampus is considered most orthologous to the MB in flies as neurons of both are critical for associative learning and circadian rythms.[74] Fittingly, *Tnpo1/2* activity impacts circadian rhythms in mice[53,103] and proband 15 has sleep disturbance. Attention deficit disorder (ADD) and autism spectrum disorder (ASD), which are seen in the majority of our cohort, are commonly associated with sleep deficits.[104] Further, our data show that *dTnpo* reduction in mature neurons disrupts their function and survival of the flies (see Figure 4). This may be the result of many of its cargoes being important neuronal proteins including FET proteins[105] (FUS,[14] EWS [MIM: 133450],[106] TAF15 [MIM: 601574]), HuR/ElavL1,[8,11,15,16] hnRNPA1,[8,17] and Huntington (HTT

[MIM: 613004]).[107] Thus, perturbations to the translocation of these and other ubiquitous cargoes into the nucleus due to disrupted *TNPO1/2* activity are likely to contribute to neurotoxicity. In fact, HuR and FUS have been implicated in ASD[108,109] and FET proteins in ADD.[110] It is also notable that homozygous null *Tnpo2* mice are viable but may have significant anxiety and locomotion abnormalities.[111] Mouse phenotypes are likely weaker than fly phenotypes because of compensation from *Tnpo1* for *Tnpo2* loss.

Overall, current data support that disruptions to *TNPO2* activity can contribute to GDD, intellectual disability, behavioral deficits, and neurologic features observed in our cohort (see Tables 1 and S1).

Potential genetic interactions

As TNPO2 is shown to be a dosage dependent and pleiotropic protein, an individual's unique genetic profile may contribute to disease occurrence and presentation. Interestingly, probands 5, 6, and 15 carry heterozygous variants of uncertain significance (VUSs) in genes highly expressed in the brain and predicted to be involved in neurological pathways, including *CUX2* (a transcription factor involved in neuron proliferation, differentiation, and synaptic plasticity[112,113]), *ANKFY1* (likely involved in vesicle trafficking[114] and required for murine brain development[115]), and *INA* (a class IV neuronal intermediate filament involved in neuron morphogenesis[116]) (see Note S1). Thus, there is potential for genetic interactions between heterozygous loss of these genes and *TNPO2* variants. Further, proband 8 carries a VUS in *ARCMC9* which is associated with Joubert syndrome 30 (JBTS30).[117] Joubert syndrome is an autosomal-recessive disorder which also involves GDD, ophthalmologic abnormalities, dysmorphic features, and hypotonia. The protein encoded by *ARCMC9* impacts ciliogenesis like TNPO1/2.[20–22,117] Thus, heterozygous loss of this gene could contribute to *TNPO2*-associated phenotypes. Last, proband 14 carries a *de novo* SNV in *PDE4D* which is predicted to cause a truncation and nonsense-mediated decay. Accordingly, this individual is diagnosed with acrodysostosis 2.[56] We hypothesize that the *TNPO2* variant in this individual contributes to developmental delays.

Concluding remarks

Overall, our data show that *TNPO2*-associated disorder represents a rare genetic condition with global developmental delay and syndromic features. As both upregulation and downregulation of *Transportin* causes similar defects in the fly and coding variants may increase or decrease *hTNPO2*'s activity, it is difficult to differentiate symptoms associated with a gain- or loss-of-function variant in individuals within our cohort. We conclude that because of pleiotropic effects of *TNPO2* variants, sequencing and phenotypic comparison to reported cases is the most valuable approach to diagnosing features related to *TNPO2*. Further examination of these and additional cases will likely delineate the genotype-phenotype correlation.

Data and code availability

This study did not generate datasets. All reagents developed in this study are available upon request.

Supplemental information

Supplemental information can be found online at https://doi.org/10.1016/j.ajhg.2021.06.019.

Acknowledgments

We thank all members of our cohort and their families for agreeing to participate in this study. We thank former and present Bellen, Wangler, and Yamamoto lab members for their input during investigations, particularly Akhila Rajan, David Li-Kroger, Paul C. Marcogliese, Yiming Zu, and Guang Lin. We thank Anthony (Ton) J. van Essen, who unfortunately passed away before this manuscript was compiled, for his initial work with proband 11. Thank you to Hervé Tricoire and Nancy M. Bonini for copies of the *da-GAL4*^{GS} fly line. *Drosophila* stock centers have been instrumental to these studies and include Bloomington Drosophila Stock Center, Vienna Drosophila Research Center, and Kyoto Stock Center. Research reported in this manuscript was supported by the National Institutes of Health (NIH) Common Fund, through the Office of Strategic Coordination/Office of the NIH Director under award numbers U54 NS093793 and U01 HG007672. Further support came from NIH award R24 OD02205, NIH award R01 GM067858, and HHMI to H.J.B. L.D.G. was supported by NIH training grant T32 NS043124-18. Research reported in this publication was supported by the Eunice Kennedy Shriver National Institute of Child Health & Human Development of the NIH award P50 HD103555 for use of the Neurovisualization Core facility. The content is solely the responsibility of the authors and does not necessarily represent the official views of the NIH. W.-L.C. was supported by Taiwan Merit Scholarships Program sponsored by the National Science Council, award NSC-095-SAF-I-564-015-TMS. M.A.K. and D.S. were supported by a NIHR Professorship. M.A.K. and K.E.S.B. were supported by the Sir Jules Thorn Award for Biomedical Research and Rosetrees Trust. S.S.M. was supported by the Cerebral Palsy Alliance, Australia (award PG01217).

Declaration of interests

The Department of Molecular and Human Genetics at Baylor College of Medicine receives revenue from clinical genetic testing completed at Baylor Genetics Laboratories. Y.S. and A.B. are employees of GeneDx, Inc.

Received: January 28, 2021
Accepted: June 27, 2021
Published: July 26, 2021

Web resources

CADD, https://cadd.gs.washington.edu/
ClinVar, https://www.ncbi.nlm.nih.gov/clinvar/
DIOPT, https://www.flyrnai.org/cgi-bin/DRSC_orthologs.pl

GenBank, https://www.ncbi.nlm.nih.gov/genbank/
GeneMatcher (accessed December 2020), https://genematcher.org/
gnomAD Browser, v.2.1.1, https://gnomad.broadinstitute.org/
MARRVEL, http://marrvel.org/
OMIM, https://www.omim.org/

References

1. Wangler, M.F., Yamamoto, S., Chao, H.-T., Posey, J.E., Westerfield, M., Postlethwait, J., Hieter, P., Boycott, K.M., Campeau, P.M., Bellen, H.J.; and Members of the Undiagnosed Diseases Network (UDN) (2017). Model Organisms Facilitate Rare Disease Diagnosis and Therapeutic Research. Genetics *207*, 9–27.
2. Bellen, H.J., Wangler, M.F., and Yamamoto, S. (2019). The fruit fly at the interface of diagnosis and pathogenic mechanisms of rare and common human diseases. Hum. Mol. Genet. *28* (R2), R207–R214.
3. Ittisoponpisan, S., Alhuzimi, E., Sternberg, M.J.E., and David, A. (2017). Landscape of Pleiotropic Proteins Causing Human Disease: Structural and System Biology Insights. Hum. Mutat. *38*, 289–296.
4. Brown, S.D.M., and Lad, H.V. (2019). The dark genome and pleiotropy: challenges for precision medicine. Mamm. Genome *30*, 212–216.
5. Twyffels, L., Gueydan, C., and Kruys, V. (2014). Transportin-1 and Transportin-2: protein nuclear import and beyond. FEBS Lett. *588*, 1857–1868.
6. Prpar Mihevc, S., Darovic, S., Kovanda, A., Bajc Česnik, A., Župunski, V., and Rogelj, B. (2017). Nuclear trafficking in amyotrophic lateral sclerosis and frontotemporal lobar degeneration. Brain *140*, 13–26.
7. Cavazza, T., and Vernos, I. (2016). The RanGTP Pathway: From Nucleo-Cytoplasmic Transport to Spindle Assembly and Beyond. Front. Cell Dev. Biol. *3*, 82.
8. Rebane, A., Aab, A., and Steitz, J.A. (2004). Transportins 1 and 2 are redundant nuclear import factors for hnRNP A1 and HuR. RNA *10*, 590–599.
9. Quan, Y., Ji, Z.-L., Wang, X., Tartakoff, A.M., and Tao, T. (2008). Evolutionary and transcriptional analysis of karyopherin β superfamily proteins. Mol. Cell. Proteomics *7*, 1254–1269.
10. Hock, E.-M., Maniecka, Z., Hruska-Plochan, M., Reber, S., Laferrière, F., Sahadevan M K, S., Ederle, H., Gittings, L., Pelkmans, L., Dupuis, L., et al. (2018). Hypertonic Stress Causes Cytoplasmic Translocation of Neuronal, but Not Astrocytic, FUS due to Impaired Transportin Function. Cell Rep. *24*, 987–1000.e7.
11. van der Giessen, K., and Gallouzi, I.-E. (2007). Involvement of transportin 2-mediated HuR import in muscle cell differentiation. Mol. Biol. Cell *18*, 2619–2629.
12. Kimura, M., Morinaka, Y., Imai, K., Kose, S., Horton, P., and Imamoto, N. (2017). Extensive cargo identification reveals distinct biological roles of the 12 importin pathways. eLife *6*, e21184.
13. Mackmull, M.T., Klaus, B., Heinze, I., Chokkalingam, M., Beyer, A., Russell, R.B., Ori, A., and Beck, M. (2017). Landscape of nuclear transport receptor cargo specificity. Mol. Syst. Biol. *13*, 962.
14. Dormann, D., Rodde, R., Edbauer, D., Bentmann, E., Fischer, I., Hruscha, A., Than, M.E., Mackenzie, I.R.A., Capell, A., Schmid, B., et al. (2010). ALS-associated fused in sarcoma (FUS) mutations disrupt Transportin-mediated nuclear import. EMBO J. *29*, 2841–2857.
15. von Roretz, C., Macri, A.M., and Gallouzi, I.-E. (2011). Transportin 2 regulates apoptosis through the RNA-binding protein HuR. J. Biol. Chem. *286*, 25983–25991.
16. Güttinger, S., Mühlhäusser, P., Koller-Eichhorn, R., Brennecke, J., and Kutay, U. (2004). Transportin2 functions as importin and mediates nuclear import of HuR. Proc. Natl. Acad. Sci. USA *101*, 2918–2923.
17. Lee, B.J., Cansizoglu, A.E., Süel, K.E., Louis, T.H., Zhang, Z., and Chook, Y.M. (2006). Rules for nuclear localization sequence recognition by karyopherin β 2. Cell *126*, 543–558.
18. Hwang, B., McCool, K., Wan, J., Wuerzberger-Davis, S.M., Young, E.W.K., Choi, E.Y., Cingolani, G., Weaver, B.A., and Miyamoto, S. (2015). IPO3-mediated Nonclassical Nuclear Import of NF-κB Essential Modulator (NEMO) Drives DNA Damage-dependent NF-κB Activation. J. Biol. Chem. *290*, 17967–17984.
19. Cansizoglu, A.E., Lee, B.J., Zhang, Z.C., Fontoura, B.M.A., and Chook, Y.M. (2007). Structure-based design of a pathway-specific nuclear import inhibitor. Nat. Struct. Mol. Biol. *14*, 452–454.
20. Madugula, V., and Lu, L. (2016). A ternary complex comprising transportin1, Rab8 and the ciliary targeting signal directs proteins to ciliary membranes. J. Cell Sci. *129*, 3922–3934.
21. Dishinger, J.F., Kee, H.L., Jenkins, P.M., Fan, S., Hurd, T.W., Hammond, J.W., Truong, Y.N.-T., Margolis, B., Martens, J.R., and Verhey, K.J. (2010). Ciliary entry of the kinesin-2 motor KIF17 is regulated by importin-β2 and RanGTP. Nat. Cell Biol. *12*, 703–710.
22. Hurd, T.W., Fan, S., and Margolis, B.L. (2011). Localization of retinitis pigmentosa 2 to cilia is regulated by Importin β2. J. Cell Sci. *124*, 718–726.
23. Bernis, C., Swift-Taylor, B., Nord, M., Carmona, S., Chook, Y.M., and Forbes, D.J. (2014). Transportin acts to regulate mitotic assembly events by target binding rather than Ran sequestration. Mol. Biol. Cell *25*, 992–1009.
24. Kalab, P., and Heald, R. (2008). The RanGTP gradient - a GPS for the mitotic spindle. J. Cell Sci. *121*, 1577–1586.
25. Walther, T.C., Askjaer, P., Gentzel, M., Habermann, A., Griffiths, G., Wilm, M., Mattaj, I.W., and Hetzer, M. (2003). RanGTP mediates nuclear pore complex assembly. Nature *424*, 689–694.
26. D'Angelo, M.A., Anderson, D.J., Richard, E., and Hetzer, M.W. (2006). Nuclear pores form de novo from both sides of the nuclear envelope. Science *312*, 440–443.
27. Larrieu, D., Viré, E., Robson, S., Breusegem, S.Y., Kouzarides, T., and Jackson, S.P. (2018). Inhibition of the acetyltransferase NAT10 normalizes progeric and aging cells by rebalancing the Transportin-1 nuclear import pathway. Sci. Signal. *11*, 11.
28. Teratani, T., Tomita, K., Toma-Fukai, S., Nakamura, Y., Itoh, T., Shimizu, H., Shiraishi, Y., Sugihara, N., Higashiyama, M., Shimizu, T., et al. (2020). Redox-dependent PPARγ/Tnpo1 complex formation enhances PPARγ nuclear localization and signaling. Free Radic. Biol. Med. *156*, 45–56.
29. Putker, M., Madl, T., Vos, H.R., de Ruiter, H., Visscher, M., van den Berg, M.C.W., Kaplan, M., Korswagen, H.C., Boelens, R., Vermeulen, M., et al. (2013). Redox-dependent control of FOXO/DAF-16 by transportin-1. Mol. Cell *49*, 730–742.
30. Splinter, K., Adams, D.R., Bacino, C.A., Bellen, H.J., Bernstein, J.A., Cheatle-Jarvela, A.M., Eng, C.M., Esteves, C.,

Gahl, W.A., Hamid, R., et al.; Undiagnosed Diseases Network (2018). Effect of Genetic Diagnosis on Patients with Previously Undiagnosed Disease. N. Engl. J. Med. *379*, 2131–2139.
31. Sobreira, N., Schiettecatte, F., Valle, D., and Hamosh, A. (2015). GeneMatcher: a matching tool for connecting investigators with an interest in the same gene. Hum. Mutat. *36*, 928–930.
32. Barish, S., Barakat, T.S., Michel, B.C., Mashtalir, N., Phillips, J.B., Valencia, A.M., Ugur, B., Wegner, J., Scott, T.M., Bostwick, B., et al.; Undiagnosed Diseases Network (2020). BICRA, a SWI/SNF Complex Member, Is Associated with BAF-Disorder Related Phenotypes in Humans and Model Organisms. Am. J. Hum. Genet. *107*, 1096–1112.
33. Mao, D., Reuter, C.M., Ruzhnikov, M.R.Z., Beck, A.E., Farrow, E.G., Emrick, L.T., Rosenfeld, J.A., Mackenzie, K.M., Robak, L., Wheeler, M.T., et al.; Undiagnosed Diseases Network (2020). De novo EIF2AK1 and EIF2AK2 Variants Are Associated with Developmental Delay, Leukoencephalopathy, and Neurologic Decompensation. Am. J. Hum. Genet. *106*, 570–583.
34. Guillen Sacoto, M.J., Tchasovnikarova, I.A., Torti, E., Forster, C., Andrew, E.H., Anselm, I., Baranano, K.W., Briere, L.C., Cohen, J.S., Craigen, W.J., et al.; Undiagnosed Diseases Network (2020). De Novo Variants in the ATPase Module of MORC2 Cause a Neurodevelopmental Disorder with Growth Retardation and Variable Craniofacial Dysmorphism. Am. J. Hum. Genet. *107*, 352–363.
35. Kanca, O., Andrews, J.C., Lee, P.-T., Patel, C., Braddock, S.R., Slavotinek, A.M., Cohen, J.S., Gubbels, C.S., Aldinger, K.A., Williams, J., et al.; Undiagnosed Diseases Network (2019). De Novo Variants in WDR37 Are Associated with Epilepsy, Colobomas, Dysmorphism, Developmental Delay, Intellectual Disability, and Cerebellar Hypoplasia. Am. J. Hum. Genet. *105*, 413–424.
36. Yoon, W.H., Sandoval, H., Nagarkar-Jaiswal, S., Jaiswal, M., Yamamoto, S., Haelterman, N.A., Putluri, N., Putluri, V., Sreekumar, A., Tos, T., et al. (2017). Loss of Nardilysin, a Mitochondrial Co-chaperone for α-Ketoglutarate Dehydrogenase, Promotes mTORC1 Activation and Neurodegeneration. Neuron *93*, 115–131.
37. Liu, L., Zhang, K., Sandoval, H., Yamamoto, S., Jaiswal, M., Sanz, E., Li, Z., Hui, J., Graham, B.H., Quintana, A., and Bellen, H.J. (2015). Glial lipid droplets and ROS induced by mitochondrial defects promote neurodegeneration. Cell *160*, 177–190.
38. Tricoire, H., Battisti, V., Trannoy, S., Lasbleiz, C., Pret, A.M., and Monnier, V. (2009). The steroid hormone receptor EcR finely modulates Drosophila lifespan during adulthood in a sex-specific manner. Mech. Ageing Dev. *130*, 547–552.
39. Rajan, A., Tien, A.-C., Haueter, C.M., Schulze, K.L., and Bellen, H.J. (2009). The Arp2/3 complex and WASp are required for apical trafficking of Delta into microvilli during cell fate specification of sensory organ precursors. Nat. Cell Biol. *11*, 815–824.
40. Hayashi, S., Ito, K., Sado, Y., Taniguchi, M., Akimoto, A., Takeuchi, H., Aigaki, T., Matsuzaki, F., Nakagoshi, H., Tanimura, T., et al. (2002). GETDB, a database compiling expression patterns and molecular locations of a collection of Gal4 enhancer traps. Genesis *34*, 58–61.
41. Venken, K.J.T., He, Y., Hoskins, R.A., and Bellen, H.J. (2006). P[acman]: a BAC transgenic platform for targeted insertion of large DNA fragments in D. melanogaster. Science *314*, 1747–1751.
42. Lee, P.-T., Zirin, J., Kanca, O., Lin, W.-W., Schulze, K.L., Li-Kroeger, D., Tao, R., Devereaux, C., Hu, Y., Chung, V., et al. (2018). A gene-specific *T2A-GAL4* library for *Drosophila*. eLife *7*, e35574.
43. Bischof, J., Maeda, R.K., Hediger, M., Karch, F., and Basler, K. (2007). An optimized transgenesis system for Drosophila using germ-line-specific phiC31 integrases. Proc. Natl. Acad. Sci. USA *104*, 3312–3317.
44. Goodman, L.D., Prudencio, M., Kramer, N.J., Martinez-Ramirez, L.F., Srinivasan, A.R., Lan, M., Parisi, M.J., Zhu, Y., Chew, J., Cook, C.N., et al. (2019). Toxic expanded GGGGCC repeat transcription is mediated by the PAF1 complex in C9orf72-associated FTD. Nat. Neurosci. *22*, 863–874.
45. Ravenscroft, T.A., Janssens, J., Lee, P.-T., Tepe, B., Marcogliese, P.C., Makhzami, S., Holmes, T.C., Aerts, S., and Bellen, H.J. (2020). *Drosophila* Voltage-Gated Sodium Channels Are Only Expressed in Active Neurons and Are Localized to Distal Axonal Initial Segment-like Domains. J. Neurosci. *40*, 7999–8024.
46. Link, N., Chung, H., Jolly, A., Withers, M., Tepe, B., Arenkiel, B.R., Shah, P.S., Krogan, N.J., Aydin, H., Geckinli, B.B., et al. (2019). Mutations in ANKLE2, a ZIKA Virus Target, Disrupt an Asymmetric Cell Division Pathway in Drosophila Neuroblasts to Cause Microcephaly. Dev. Cell *51*, 713–729.e6.
47. Goodman, L.D., Prudencio, M., Srinivasan, A.R., Rifai, O.M., Lee, V.M.-Y., Petrucelli, L., and Bonini, N.M. (2019). eIF4B and eIF4H mediate GR production from expanded G4C2 in a Drosophila model for C9orf72-associated ALS. Acta Neuropathol. Commun. *7*, 62.
48. Wang, J., Al-Ouran, R., Hu, Y., Kim, S.-Y., Wan, Y.-W., Wangler, M.F., Yamamoto, S., Chao, H.-T., Comjean, A., Mohr, S.E., et al.; UDN (2017). MARRVEL: Integration of Human and Model Organism Genetic Resources to Facilitate Functional Annotation of the Human Genome. Am. J. Hum. Genet. *100*, 843–853.
49. Samocha, K.E., Robinson, E.B., Sanders, S.J., Stevens, C., Sabo, A., McGrath, L.M., Kosmicki, J.A., Rehnström, K., Mallick, S., Kirby, A., et al. (2014). A framework for the interpretation of de novo mutation in human disease. Nat. Genet. *46*, 944–950.
50. Fuller, Z.L., Berg, J.J., Mostafavi, H., Sella, G., and Przeworski, M. (2019). Measuring intolerance to mutation in human genetics. Nat. Genet. *51*, 772–776.
51. Karczewski, K.J., Francioli, L.C., Tiao, G., Cummings, B.B., Alföldi, J., Wang, Q., Collins, R.L., Laricchia, K.M., Ganna, A., Birnbaum, D.P., et al.; Genome Aggregation Database Consortium (2020). The mutational constraint spectrum quantified from variation in 141,456 humans. Nature *581*, 434–443.
52. Rentzsch, P., Witten, D., Cooper, G.M., Shendure, J., and Kircher, M. (2019). CADD: predicting the deleteriousness of variants throughout the human genome. Nucleic Acids Res. *47* (D1), D886–D894.
53. Sato, M., Mizoro, Y., Atobe, Y., Fujimoto, Y., Yamaguchi, Y., Fustin, J.-M., Doi, M., and Okamura, H. (2011). Transportin 1 in the mouse brain: appearance in regions of neurogenesis, cerebrospinal fluid production/sensing, and circadian clock. J. Comp. Neurol. *519*, 1770–1780.
54. Coe, B.P., Witherspoon, K., Rosenfeld, J.A., van Bon, B.W.M., Vulto-van Silfhout, A.T., Bosco, P., Friend, K.L., Baker, C., Buono, S., Vissers, L.E.L.M., et al. (2014). Refining analyses

of copy number variation identifies specific genes associated with developmental delay. Nat. Genet. *46*, 1063–1071.
55. Lehman, A.M., McFadden, D., Pugash, D., Sangha, K., Gibson, W.T., and Patel, M.S. (2008). Schinzel-Giedion syndrome: report of splenopancreatic fusion and proposed diagnostic criteria. Am. J. Med. Genet. A. *146A*, 1299–1306.
56. Lindstrand, A., Grigelioniene, G., Nilsson, D., Pettersson, M., Hofmeister, W., Anderlid, B.-M., Kant, S.G., Ruivenkamp, C.A.L., Gustavsson, P., Valta, H., et al. (2014). Different mutations in PDE4D associated with developmental disorders with mirror phenotypes. J. Med. Genet. *51*, 45–54.
57. Allemand, E., Dokudovskaya, S., Bordonné, R., and Tazi, J. (2002). A conserved Drosophila transportin-serine/arginine-rich (SR) protein permits nuclear import of Drosophila SR protein splicing factors and their antagonist repressor splicing factor 1. Mol. Biol. Cell *13*, 2436–2447.
58. Guo, L., Kim, H.J., Wang, H., Monaghan, J., Freyermuth, F., Sung, J.C., O'Donovan, K., Fare, C.M., Diaz, Z., Singh, N., et al. (2018). Nuclear-Import Receptors Reverse Aberrant Phase Transitions of RNA-Binding Proteins with Prion-like Domains. Cell *173*, 677–692.e20.
59. Jäckel, S., Summerer, A.K., Thömmes, C.M., Pan, X., Voigt, A., Schulz, J.B., Rasse, T.M., Dormann, D., Haass, C., and Kahle, P.J. (2015). Nuclear import factor transportin and arginine methyltransferase 1 modify FUS neurotoxicity in Drosophila. Neurobiol. Dis. *74*, 76–88.
60. Shi, Q., Han, Y., and Jiang, J. (2014). Suppressor of fused impedes Ci/Gli nuclear import by opposing Trn/Kapβ2 in Hedgehog signaling. J. Cell Sci. *127*, 1092–1103.
61. Siomi, M.C., Fromont, M., Rain, J.-C., Wan, L., Wang, F., Legrain, P., and Dreyfuss, G. (1998). Functional conservation of the transportin nuclear import pathway in divergent organisms. Mol. Cell. Biol. *18*, 4141–4148.
62. Hu, Y., Flockhart, I., Vinayagam, A., Bergwitz, C., Berger, B., Perrimon, N., and Mohr, S.E. (2011). An integrative approach to ortholog prediction for disease-focused and other functional studies. BMC Bioinformatics *12*, 357.
63. Perkins, L.A., Holderbaum, L., Tao, R., Hu, Y., Sopko, R., McCall, K., Yang-Zhou, D., Flockhart, I., Binari, R., Shim, H.-S., et al. (2015). The Transgenic RNAi Project at Harvard Medical School: Resources and Validation. Genetics *201*, 843–852.
64. Dietzl, G., Chen, D., Schnorrer, F., Su, K.-C., Barinova, Y., Fellner, M., Gasser, B., Kinsey, K., Oppel, S., Scheiblauer, S., et al. (2007). A genome-wide transgenic RNAi library for conditional gene inactivation in Drosophila. Nature *448*, 151–156.
65. Singh, A., and Kango-Singh, M. (2020). Molecular Genetics of Axial Patterning, Growth and Disease in Drosophila Eye (Cham: Springer International Publishing).
66. Golic, M.M., Rong, Y.S., Petersen, R.B., Lindquist, S.L., and Golic, K.G. (1997). FLP-mediated DNA mobilization to specific target sites in Drosophila chromosomes. Nucleic Acids Res. *25*, 3665–3671.
67. Beira, J.V., and Paro, R. (2016). The legacy of Drosophila imaginal discs. Chromosoma *125*, 573–592.
68. Diaz de la Loza, M.C., and Thompson, B.J. (2017). Forces shaping the Drosophila wing. Mech. Dev. *144* (Pt A), 23–32.
69. Duffy, J.B. (2002). GAL4 system in Drosophila: a fly geneticist's Swiss army knife. Genesis *34*, 1–15.
70. Lemon, W.C., Pulver, S.R., Höckendorf, B., McDole, K., Branson, K., Freeman, J., and Keller, P.J. (2015). Whole-central nervous system functional imaging in larval Drosophila. Nat. Commun. *6*, 7924.
71. Sepp, K.J., Schulte, J., and Auld, V.J. (2001). Peripheral glia direct axon guidance across the CNS/PNS transition zone. Dev. Biol. *238*, 47–63.
72. Spokony, R.F., and Restifo, L.L. (2009). Broad Complex isoforms have unique distributions during central nervous system metamorphosis in Drosophila melanogaster. J. Comp. Neurol. *517*, 15–36.
73. Robinow, S., and White, K. (1991). Characterization and spatial distribution of the ELAV protein during Drosophila melanogaster development. J. Neurobiol. *22*, 443–461.
74. Modi, M.N., Shuai, Y., and Turner, G.C. (2020). The *Drosophila* Mushroom Body: From Architecture to Algorithm in a Learning Circuit. Annu. Rev. Neurosci. *43*, 465–484.
75. Fushima, K., and Tsujimura, H. (2007). Precise control of fasciclin II expression is required for adult mushroom body development in Drosophila. Dev. Growth Differ. *49*, 215–227.
76. Nicholson, L., Singh, G.K., Osterwalder, T., Roman, G.W., Davis, R.L., and Keshishian, H. (2008). Spatial and temporal control of gene expression in Drosophila using the inducible GeneSwitch GAL4 system. I. Screen for larval nervous system drivers. Genetics *178*, 215–234.
77. Vilinsky, I., and Johnson, K.G. (2012). Electroretinograms in Drosophila: a robust and genetically accessible electrophysiological system for the undergraduate laboratory. J. Undergrad. Neurosci. Educ. *11*, A149–A157.
78. Wang, T., and Montell, C. (2007). Phototransduction and retinal degeneration in Drosophila. Pflugers Arch. *454*, 821–847.
79. Harnish, J.M., Deal, S.L., Chao, H.-T., Wangler, M.F., and Yamamoto, S. (2019). In Vivo Functional Study of Disease-associated Rare Human Variants Using Drosophila. J. Vis. Exp. https://doi.org/10.3791/59658.
80. Nakayama, M., Ishibashi, T., Ishikawa, H.O., Sato, H., Usui, T., Okuda, T., Yashiro, H., Ishikawa, H., Taikou, Y., Minami, A., et al. (2014). A gain-of-function screen to identify genes that reduce lifespan in the adult of Drosophila melanogaster. BMC Genet. *15*, 46.
81. Li, W.-Z., Li, S.-L., Zheng, H.Y., Zhang, S.-P., and Xue, L. (2012). A broad expression profile of the GMR-GAL4 driver in Drosophila melanogaster. Genet. Mol. Res. *11*, 1997–2002.
82. Ray, M., and Lakhotia, S.C. (2015). The commonly used eye-specific sev-GAL4 and GMR-GAL4 drivers in Drosophila melanogaster are expressed in tissues other than eyes also. J. Genet. *94*, 407–416.
83. Zhang, P., Wang, Q., Hughes, H., and Intrieri, G. (2014). Synthetic Lethality Induced by a Strong *Drosophila* Enhancer of Expanded Polyglutamine Tract. OJGen *04*, 300–315.
84. de Ligt, J., Willemsen, M.H., van Bon, B.W., Kleefstra, T., Yntema, H.G., Kroes, T., Vulto-van Silfhout, A.T., Koolen, D.A., de Vries, P., Gilissen, C., et al. (2012). Diagnostic exome sequencing in persons with severe intellectual disability. N. Engl. J. Med. *367*, 1921–1929.
85. Lelieveld, S.H., Reijnders, M.R.F., Pfundt, R., Yntema, H.G., Kamsteeg, E.-J., de Vries, P., de Vries, B.B.A., Willemsen, M.H., Kleefstra, T., Löhner, K., et al. (2016). Meta-analysis of 2,104 trios provides support for 10 new genes for intellectual disability. Nat. Neurosci. *19*, 1194–1196.
86. McRae, J.F., Clayton, S., Fitzgerald, T.W., Kaplanis, J., Prigmore, E., Rajan, D., Sifrim, A., Aitken, S., Akawi, N.; and Deciphering Developmental Disorders Study (2017). Prevalence and architecture of de novo mutations in developmental disorders. Nature *542*, 433–438.

87. Grozeva, D., Carss, K., Spasic-Boskovic, O., Tejada, M.-I., Gecz, J., Shaw, M., Corbett, M., Haan, E., Thompson, E., Friend, K., et al.; Italian X-linked Mental Retardation Project; UK10K Consortium; GOLD Consortium (2015). Targeted Next-Generation Sequencing Analysis of 1,000 Individuals with Intellectual Disability. Hum. Mutat. *36*, 1197–1204.
88. Barbato, S., Kapinos, L.E., Rencurel, C., and Lim, R.Y.H. (2020). Karyopherin enrichment at the nuclear pore complex attenuates Ran permeability. J. Cell Sci. *133*, 133.
89. Lam, W.W.K., Millichap, J.J., Soares, D.C., Chin, R., McLellan, A., FitzPatrick, D.R., Elmslie, F., Lees, M.M., Schaefer, G.B., Abbott, C.M.; and DDD study (2016). Novel de novo EEF1A2 missense mutations causing epilepsy and intellectual disability. Mol. Genet. Genomic Med. *4*, 465–474.
90. Landrum, M.J., Lee, J.M., Benson, M., Brown, G.R., Chao, C., Chitipiralla, S., Gu, B., Hart, J., Hoffman, D., Jang, W., et al. (2018). ClinVar: improving access to variant interpretations and supporting evidence. Nucleic Acids Res. *46* (D1), D1062–D1067.
91. Kaminsky, E.B., Kaul, V., Paschall, J., Church, D.M., Bunke, B., Kunig, D., Moreno-De-Luca, D., Moreno-De-Luca, A., Mulle, J.G., Warren, S.T., et al. (2011). An evidence-based approach to establish the functional and clinical significance of copy number variants in intellectual and developmental disabilities. Genet. Med. *13*, 777–784.
92. Miller, D.T., Adam, M.P., Aradhya, S., Biesecker, L.G., Brothman, A.R., Carter, N.P., Church, D.M., Crolla, J.A., Eichler, E.E., Epstein, C.J., et al. (2010). Consensus statement: chromosomal microarray is a first-tier clinical diagnostic test for individuals with developmental disabilities or congenital anomalies. Am. J. Hum. Genet. *86*, 749–764.
93. Janiszewska, M., De Vito, C., Le Bitoux, M.-A., Fusco, C., and Stamenkovic, I. (2010). Transportin regulates nuclear import of CD44. J. Biol. Chem. *285*, 30548–30557.
94. Kimura, M., Kose, S., Okumura, N., Imai, K., Furuta, M., Sakiyama, N., Tomii, K., Horton, P., Takao, T., and Imamoto, N. (2013). Identification of cargo proteins specific for the nucleocytoplasmic transport carrier transportin by combination of an in vitro transport system and stable isotope labeling by amino acids in cell culture (SILAC)-based quantitative proteomics. Mol. Cell. Proteomics *12*, 145–157.
95. Arnold, M., Nath, A., Wohlwend, D., and Kehlenbach, R.H. (2006). Transportin is a major nuclear import receptor for c-Fos: a novel mode of cargo interaction. J. Biol. Chem. *281*, 5492–5499.
96. Malnou, C.E., Salem, T., Brockly, F., Wodrich, H., Piechaczyk, M., and Jariel-Encontre, I. (2007). Heterodimerization with Jun family members regulates c-Fos nucleocytoplasmic traffic. J. Biol. Chem. *282*, 31046–31059.
97. Waldmann, I., Wälde, S., and Kehlenbach, R.H. (2007). Nuclear import of c-Jun is mediated by multiple transport receptors. J. Biol. Chem. *282*, 27685–27692.
98. Hasselblatt, P., Gresh, L., Kudo, H., Guinea-Viniegra, J., and Wagner, E.F. (2008). The role of the transcription factor AP-1 in colitis-associated and β-catenin-dependent intestinal tumorigenesis in mice. Oncogene *27*, 6102–6109.
99. Nenci, A., Becker, C., Wullaert, A., Gareus, R., van Loo, G., Danese, S., Huth, M., Nikolaev, A., Neufert, C., Madison, B., et al. (2007). Epithelial NEMO links innate immunity to chronic intestinal inflammation. Nature *446*, 557–561.
100. Qiu, W., Wang, X., Buchanan, M., He, K., Sharma, R., Zhang, L., Wang, Q., and Yu, J. (2013). ADAR1 is essential for intestinal homeostasis and stem cell maintenance. Cell Death Dis. *4*, e599–e599.
101. Fritz, J., Strehblow, A., Taschner, A., Schopoff, S., Pasierbek, P., and Jantsch, M.F. (2009). RNA-regulated interaction of transportin-1 and exportin-5 with the double-stranded RNA-binding domain regulates nucleocytoplasmic shuttling of ADAR1. Mol. Cell. Biol. *29*, 1487–1497.
102. Samborski, P., and Grzymisławski, M. (2015). The Role of HSP70 Heat Shock Proteins in the Pathogenesis and Treatment of Inflammatory Bowel Diseases. Adv. Clin. Exp. Med. *24*, 525–530.
103. Korge, S., Maier, B., Brüning, F., Ehrhardt, L., Korte, T., Mann, M., Herrmann, A., Robles, M.S., and Kramer, A. (2018). The non-classical nuclear import carrier Transportin 1 modulates circadian rhythms through its effect on PER1 nuclear localization. PLoS Genet. *14*, e1007189.
104. Singh, K., and Zimmerman, A.W. (2015). Sleep in Autism Spectrum Disorder and Attention Deficit Hyperactivity Disorder. Semin. Pediatr. Neurol. *22*, 113–125.
105. Dormann, D., Madl, T., Valori, C.F., Bentmann, E., Tahirovic, S., Abou-Ajram, C., Kremmer, E., Ansorge, O., Mackenzie, I.R.A., Neumann, M., and Haass, C. (2012). Arginine methylation next to the PY-NLS modulates Transportin binding and nuclear import of FUS. EMBO J. *31*, 4258–4275.
106. Leemann-Zakaryan, R.P., Pahlich, S., Grossenbacher, D., and Gehring, H. (2011). Tyrosine Phosphorylation in the C-Terminal Nuclear Localization and Retention Signal (C-NLS) of the EWS Protein. Sarcoma *2011*, 218483. https://doi.org/10.1155/2011/218483.
107. Desmond, C.R., Atwal, R.S., Xia, J., and Truant, R. (2012). Identification of a karyopherin β1/β2 proline-tyrosine nuclear localization signal in huntingtin protein. J. Biol. Chem. *287*, 39626–39633.
108. Popovitchenko, T., Thompson, K., Viljetic, B., Jiao, X., Kontonyiannis, D.L., Kiledjian, M., Hart, R.P., and Rasin, M.R. (2016). The RNA binding protein HuR determines the differential translation of autism-associated FoxP subfamily members in the developing neocortex. Sci. Rep. *6*, 28998.
109. Ho, W.Y., Chang, J.-C., Tyan, S.-H., Yen, Y.-C., Lim, K., Tan, B.S.Y., Ong, J., Tucker-Kellogg, G., Wong, P., Koo, E., and Ling, S.C. (2019). FUS-mediated dysregulation of Sema5a, an autism-related gene, in FUS mice with hippocampus-dependent cognitive deficits. Hum. Mol. Genet. *28*, 3777–3791.
110. Kino, Y., Washizu, C., Kurosawa, M., Yamada, M., Miyazaki, H., Akagi, T., Hashikawa, T., Doi, H., Takumi, T., Hicks, G.G., et al. (2015). FUS/TLS deficiency causes behavioral and pathological abnormalities distinct from amyotrophic lateral sclerosis. Acta Neuropathol. Commun. *3*, 24.
111. Koscielny, G., Yaikhom, G., Iyer, V., Meehan, T.F., Morgan, H., Atienza-Herrero, J., Blake, A., Chen, C.-K., Easty, R., Di Fenza, A., et al. (2014). The International Mouse Phenotyping Consortium Web Portal, a unified point of access for knockout mice and related phenotyping data. Nucleic Acids Res. *42*, D802–D809.
112. Barington, M., Risom, L., Ek, J., Uldall, P., and Ostergaard, E. (2018). A recurrent de novo CUX2 missense variant associated with intellectual disability, seizures, and autism spectrum disorder. Eur. J. Hum. Genet. *26*, 1388–1391.
113. Cubelos, B., Sebastián-Serrano, A., Beccari, L., Calcagnotto, M.E., Cisneros, E., Kim, S., Dopazo, A., Alvarez-Dolado, M., Redondo, J.M., Bovolenta, P., et al. (2010). Cux1 and Cux2 regulate dendritic branching, spine morphology, and

synapses of the upper layer neurons of the cortex. Neuron *66*, 523–535.

114. Kuriyama, H., Asakawa, S., Minoshima, S., Maruyama, H., Ishii, N., Ito, K., Gejyo, F., Arakawa, M., Shimizu, N., and Kuwano, R. (2000). Characterization and chromosomal mapping of a novel human gene, ANKHZN. Gene *253*, 151–160.
115. Ding, M., Weng, C., Fan, S., Cao, Q., and Lu, Z. (2017). Purkinje Cell Degeneration and Motor Coordination Deficits in a New Mouse Model of Autosomal Recessive Spastic Ataxia of Charlevoix-Saguenay. Front. Mol. Neurosci. *10*, 121.
116. Bott, C.J., and Winckler, B. (2020). Intermediate filaments in developing neurons: Beyond structure. Cytoskeleton (Hoboken) *77*, 110–128.
117. Van De Weghe, J.C., Rusterholz, T.D.S., Latour, B., Grout, M.E., Aldinger, K.A., Shaheen, R., Dempsey, J.C., Maddirevula, S., Cheng, Y.-H.H., Phelps, I.G., et al.; University of Washington Center for Mendelian Genomics (2017). Mutations in ARMC9, which Encodes a Basal Body Protein, Cause Joubert Syndrome in Humans and Ciliopathy Phenotypes in Zebrafish. Am. J. Hum. Genet. *101*, 23–36.

The American Journal of Human Genetics, Volume *108*

Supplemental information

TNPO2 variants associate with human developmental delays, neurologic deficits, and dysmorphic features and alter *TNPO2* activity in *Drosophila*

Lindsey D. Goodman, Heidi Cope, Zelha Nil, Thomas A. Ravenscroft, Wu-Lin Charng, Shenzhao Lu, An-Chi Tien, Rolph Pfundt, David A. Koolen, Charlotte A. Haaxma, Hermine E. Veenstra-Knol, Jolien S. Klein Wassink-Ruiter, Marijke R. Wevers, Melissa Jones, Laurence E. Walsh, Victoria H. Klee, Miel Theunis, Eric Legius, Dora Steel, Katy E.S. Barwick, Manju A. Kurian, Shekeeb S. Mohammad, Russell C. Dale, Paulien A. Terhal, Ellen van Binsbergen, Brian Kirmse, Bethany Robinette, Benjamin Cogné, Bertrand Isidor, Theresa A. Grebe, Peggy Kulch, Bryan E. Hainline, Katherine Sapp, Eva Morava, Eric W. Klee, Erica L. Macke, Pamela Trapane, Christopher Spencer, Yue Si, Amber Begtrup, Matthew J. Moulton, Debdeep Dutta, Oguz Kanca, Undiagnosed Diseases Network, Michael F. Wangler, Shinya Yamamoto, Hugo J. Bellen, and Queenie K.-G. Tan

Supplemental Note S1: Case reports.

Proband 5 carries three *de novo,* heterozygous VUS in addition to the reported variant in *TNPO2*. First, is a frameshift variant in *SET binding protein 1* (*SETBP1*; NM_015559): c.4565delinsGGC (p.Leu1522Argfs*59). *SETBP1* encodes a DNA-binding protein that is involved in chromatin dynamics and gene expression. *SETBP1* is a highly constrained gene – misZ=1.10 (o/e=0.90), pLI=1.00 (o/e=0.02) – and has been associated with mental retardation, autosomal dominant 29 (MIM: 616078) and Schinzel-Giedion midface retraction syndrome; autosomal dominant (MIM: 269150). Importantly, this variant is considerably further down in the gene than known pathogenic variants[1], falling within the last exon in the canonical transcript about 70 amino acids from the end. Further, the proband has no features suggestive of Schinzel-Giedion syndrome[2]. A second, *de novo*, heterozygous SNV is detected in *Cut-like Homeobox 2* (*CUX2*; NM_015267):c.3758A>C (p.His1253Pro). *CUX2* is highly constrained – misZ=3.18 (o/e=0.70), pLI=1.00 (o/e=0.09) – and has been associated with developmental and epileptic encephalopathy 67 (MIM: 618141; autosomal dominant). *CUX2* encodes a transcription factor involved in neuron morphogenesis and synaptic plasticity. Variants in the gene have recently been associated with rare cases involving intellectual disability, seizures and ASD[3]. However, the variant in our proband is not predicted to be pathogenic by SIFT, PolyPhen and Align GVGD and is associated with a CADD score of 17.1. As this individual's *TNPO2* variant causes a deletion at an amino acid conserved in mammals, the *TNPO2* variant is the primary candidate to explain the individual's features, and the mosacism may explain the proband's relatively mild features. The last VUS detected in our proband is a 12q13.13 duplication that was determined to unlikely be clinically relevant. Overall, the proband's variant in *TNPO2* was the most likely candidate for further study.

Proband 6 carries a *de novo,* heterozygous deletion/insertion in *Rabankyrin-5* (*ANKFY1;* NM_001257999.2): c.3263delinsGCT (p.Thr1088Serfs*9) in addition to the reported variant in *TNPO2*. *ANKFY1* is a moderately constrained gene – misZ= 2.46 (o/e=0.74), pLI= 0.96 (o/e=0.19) – that has not been associated with Mendelian disease. *ANKFY1* encodes a cytoplasmic protein that is predicted to be involved in vesicle or protein transport. Given the relatively lower gene constraint compared to *TNPO2*, this variant is not the primary candidate for further investigation to explain the proband's features.

Proband 8 carries a *de novo,* heterozygous SNV in *Armadillo repeat containing 9* (*ARMC9;* NM_025139.3):c.988G>A (p.Asp330Asn) in addition to a TNPO2 variant. The ARMC9 variant has a CADD score of 24 and is not found in gnomAD. This gene is lowly constrained – misZ=0.85 (o/e=0.88), pLI=0.00 (o/e=0.78) – while variants in *ARMC9* have been associated with the autosomal recessive Joubert syndrome 30 (MIM: 617622). Given the low constraint of this gene and the presence of only one variant in an autosomal recessive disorder, it is not the primary candidate to explain this individual's symptoms.

Proband 10 carries three *de novo,* heterozygous CNVs (two micro-insertions and one micro-deletion) and three *de novo,* heterozygous SNVs in genes with lower constraint than *TNPO2* in addition to the reported *TNPO2* variant. The most notable of these is a 522 Kb gain at 1q21.1 (1:g.145,287,319-145,809,279)x3). Genes impacted by these VUS are not associated with disease and do not explain the individual's symptoms. Overall, these VUS were not considered the explanation for the proband's features.

Proband 14 carries a *de novo,* heterozygous SNV in *Phosphodiesterase-4D* (*PDE4D;* NM_001104631.1): c.709C>T (p.Arg237*) in addition to the reported variant in *TNPO2*. The *PDE4D* variant corresponds to a CADD score of 37.0 and is not found in gnomAD. The gene is highly constrained – misZ=3.75 (o/e=0.47), pLI= 1.00, (o/e=0.08). *PDE4D* encodes a cAMP phosphodiesterase that mediates cAMP degradation and plays a critical roles in synaptic

plasticity and development. Variants within *PDE4D* are associated with acrodysostosis 2 (ACRDYS2 [MIM: 614613]) and truncating variants are associated with an intellectual disability (ID) syndrome[4]. The features of this proband is thought to be consistent with *PED4D*-associated ID syndrome, but the *de novo TNPO2* variant likely plays an additive role in his disease presentation.

Proband 15 carries a *de novo,* heterozygous SNV in *α-Internexin* (*INA*; NM_032727.4): c.1127T>C (p.Leu376Pro) that is mosaic (20% of reads) in addition to the reported variant in *TNPO2*. This *INA* variant has a CADD score of 30.0, is not found in gnomAD, and has not been associated with a Mendelian disease. Because INA is a lowly constrained gene – misZ= 2.13 (o/e=0.63), pLI= 0.00 (o/e=0.88) – and this variant is mosaic, it is not the primary candidate to explain the proband's symptoms. *INA* encodes a Class-IV neuronal intermediate filament and is not currently known to be associated with human disease.

Supplemental Note S2: UDN consortia co-investigators

The Undiagnosed Diseases Network (UDN) co-investigators are Maria T. Acosta, Margaret Adam, David R. Adams, Pankaj B. Agrawal, Mercedes E. Alejandro, Justin Alvey, Laura Amendola, Ashley Andrews, Euan A. Ashley, Mahshid S. Azamian, Carlos A. Bacino, Guney Bademci, Eva Baker, Ashok Balasubramanyam, Dustin Baldridge, Jim Bale, Michael Bamshad, Deborah Barbouth, Pinar Bayrak-Toydemir, Anita Beck, Alan H. Beggs, Edward Behrens, Gill Bejerano, Jimmy Bennet, Beverly Berg-Rood, Jonathan A. Bernstein, Gerard T. Berry, Anna Bican, Stephanie Bivona, Elizabeth Blue, John Bohnsack, Carsten Bonnenmann, Devon Bonner, Lorenzo Botto, Brenna Boyd, Lauren C. Briere, Elly Brokamp, Gabrielle Brown, Elizabeth A. Burke, Lindsay C. Burrage, Manish J. Butte, Peter Byers, William E. Byrd, John Carey, Olveen Carrasquillo, Ta Chen Peter Chang, Sirisak Chanprasert, Hsiao-Tuan Chao, Gary D. Clark, Terra R. Coakley, Laurel A. Cobban, Joy D. Cogan, Matthew Coggins, F. Sessions Cole, Heather A. Colley, Cynthia M. Cooper, Heidi Cope, William J. Craigen, Andrew B. Crouse, Michael Cunningham, Precilla D'Souza, Hongzheng Dai, Surendra Dasari, Joie Davis, Jyoti G. Dayal, Matthew Deardorff, Esteban C. Dell'Angelica, Shweta U. Dhar, Katrina Dipple, Daniel Doherty, Naghmeh Dorrani, Argenia L. Doss, Emilie D. Douine, David D. Draper, Laura Duncan, Dawn Earl, David J. Eckstein, Lisa T. Emrick, Christine M. Eng, Cecilia Esteves, Marni Falk, Liliana Fernandez, Carlos Ferreira, Elizabeth L. Fieg, Laurie C. Findley, Paul G. Fisher, Brent L. Fogel, Irman Forghani, William A. Gahl, Ian Glass, Bernadette Gochuico, Rena A. Godfrey, Katie Golden-Grant, Alica M. Goldman, Madison P. Goldrich, David B. Goldstein, Alana Grajewski, Catherine A. Groden, Irma Gutierrez, Sihoun Hahn, Rizwan Hamid, Neil A. Hanchard, Athena Hantzaridis, Kelly Hassey, Nichole Hayes, Frances High, Anne Hing, Fuki M. Hisama, Ingrid A. Holm, Jason Hom, Martha Horike-Pyne, Alden Huang, Yong Huang, Laryssa Huryn, Rosario Isasi, Fariha Jamal, Gail P. Jarvik, Jeffrey Jarvik, Suman Jayadev, Lefkothea Karaviti, Jennifer Kennedy, Dana Kiley, Shilpa N. Kobren, Isaac S. Kohane, Jennefer N. Kohler, Deborah Krakow, Donna M. Krasnewich, Elijah Kravets, Susan Korrick, Mary Koziura, Joel B. Krier, Seema R. Lalani, Byron Lam, Christina Lam, Grace L. LaMoure, Brendan C. Lanpher, Ian R. Lanza, Lea Latham, Kimberly LeBlanc, Brendan H. Lee, Hane Lee, Roy Levitt, Richard A. Lewis, Sharyn A. Lincoln, Pengfei Liu, Xue Zhong Liu, Nicola Longo, Sandra K. Loo, Joseph Loscalzo, Richard L. Maas, John MacDowall, Ellen F. Macnamara, Calum A. MacRae, Valerie V. Maduro, Bryan C. Mak, May Christine V. Malicdan, Laura A. Mamounas, Teri A. Manolio, Rong Mao, Kenneth Maravilla, Thomas C. Markello, Ronit Marom, Gabor Marth, Beth A. Martin, Martin G. Martin, Julian A. Martínez-Agosto, Shruti Marwaha, Jacob McCauley, Allyn McConkie-Rosell, Alexa T. McCray, Elisabeth McGee, Heather Mefford, J. Lawrence Merritt, Matthew Might, Ghayda Mirzaa, Eva Morava, Paolo M. Moretti, Deborah Mosbrook-Davis, John J. Mulvihill, David R. Murdock, Anna Nagy, Mariko Nakano-Okuno, Avi Nath, Stan F. Nelson, John H. Newman, Sarah K. Nicholas, Deborah Nickerson, Shirley Nieves-Rodriguez, Donna Novacic, Devin Oglesbee, James P. Orengo, Laura Pace, Stephen Pak, J. Carl Pallais, Christina GS. Palmer, Jeanette C. Papp, Neil H. Parker, John A. Phillips III, Jennifer E. Posey, Lorraine Potocki, Bradley Power, Barbara N. Pusey, Aaron Quinlan, Wendy Raskind, Archana N. Raja, Deepak A. Rao, Genecee Renteria, Chloe M. Reuter, Lynette Rives, Amy K. Robertson, Lance H. Rodan, Jill A. Rosenfeld, Natalie Rosenwasser, Francis Rossignol, Maura Ruzhnikov, Ralph Sacco, Jacinda B. Sampson, Susan L. Samson, Mario Saporta, C. Ron Scott, Judy Schaechter, Timothy Schedl, Kelly Schoch, Daryl A. Scott, Vandana Shashi, Jimann Shin, Rebecca Signer, Edwin K. Silverman, Janet S. Sinsheimer, Kathy Sisco, Edward C. Smith, Kevin S. Smith, Emily Solem, Lilianna Solnica-Krezel, Ben Solomon, Rebecca C. Spillmann, Joan M. Stoler, Jennifer A. Sullivan, Kathleen Sullivan, Angela Sun, Shirley Sutton, David A. Sweetser, Virginia Sybert, Holly K. Tabor, Amelia L. M. Tan, Queenie K.-G.Tan, Mustafa Tekin, Fred Telischi, Willa Thorson, Audrey Thurm, Cynthia J. Tifft, Camilo Toro, Alyssa A. Tran, Brianna M. Tucker, Tiina K. Urv, Adeline Vanderver, Matt Velinder, Dave Viskochil, Tiphanie P. Vogel, Colleen E. Wahl,

Stephanie Wallace, Nicole M. Walley, Chris A. Walsh, Melissa Walker, Jennifer Wambach, Jijun Wan, Lee-kai Wang, Michael F. Wangler, Patricia A. Ward, Daniel Wegner, Mark Wener, Tara Wenger, Katherine Wesseling Perry, Monte Westerfield, Matthew T. Wheeler, Jordan Whitlock, Lynne A. Wolfe, Jeremy D. Woods, Shinya Yamamoto, John Yang, Muhammad Yousef, Diane B. Zastrow, Wadih Zein, Chunli Zhao, Stephan Zuchner.

A ***dTnpo* Knockdown**

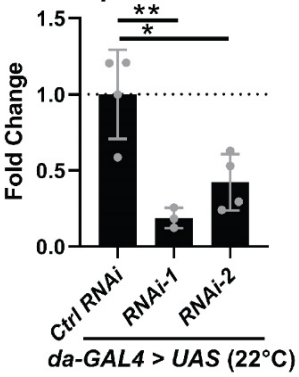

B **Stage of death with RNAi**

25°C	*da-GAL4*
dTnpo RNAi-1	L2*
dTnpo RNAi-2	L3*

* in rare cases escaper puparia are observed

C ***nub-GAL4* (25°C), lethal with RNAi-1**

D ***ey-GAL4* (~22°C), lethal with RNAi-1**

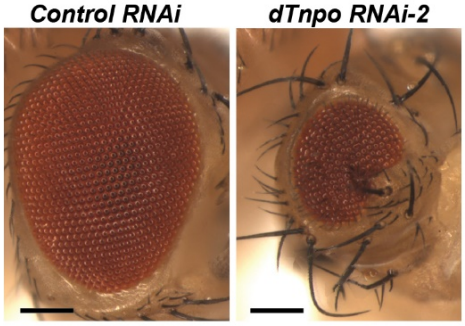

E ***GMR-GAL4* (25°C)**

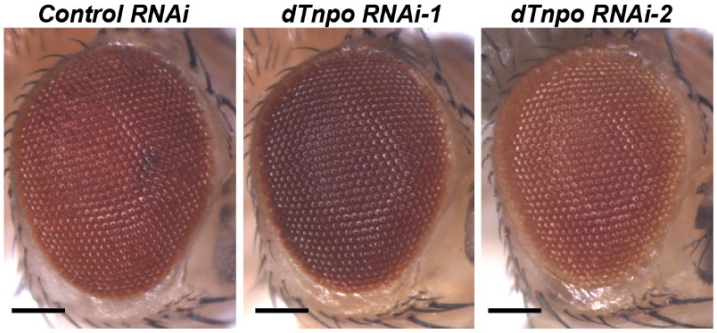

F **Summary of effects when *dTnpo* is downregulated in specific tissues using *GAL4 > UAS-RNAi***

GAL4 Driver	Primary Tissue(s)	Stage	*UAS-dTnpo RNAi-1*	*UAS-dTnpo RNAi-2*
Ubiquitous				
daughterless (da)-GAL4	ubiquitous	embryonic-adult	Larval lethal (18-29°C): L2 at 25°C	Larval lethal (25°C); pupal lethal (22°C)
daughterless (da)-GAL4[GS]	ubiquitous	adult (drug-induced)	reduced lifespan (29°C)	n/a
Nervous system				
inscuteable (insc)-GAL4	neuroblasts	embryonic	no obvious phenotypes (25°C)	no obvious phenotypes (25°C)
elav-GAL4	neurons	embryonic-adult	Lethal: larval at 29°C, pupal at ≤25°C	no obvious phenotype (≤29°C, 10d)
elav-GAL4[GS]	neurons	adult (drug-induced)	reduced lifespan (29°C)	n/a
Optic system				
eyeless (ey)-GAL4	developing eye	embryonic-adult	Larval lethal (25°C); pupal lethal (≤22°C)	morphological defects (18-29°C)*,#
GMR-GAL4 (Glass)	developing retina, photorecepter cells	3rd instar-adult	no external eye phenotype (25°C)	no external eye phenotype (25°C)
Rh1-GAL4 (NinaE)	photoreceptor neurons	adult	ERG defects at 7d (29°C)	mild ERG defects at 22d (29°C)
Thorax				
nubbin (nub)-GAL4	ventral thoracic disc, wing disc, haltere disc	embryonic-adult	Lethal: larval at 25°C, pupal at 22°C**	severe wing and haltere phenotypes (22-25°C)*
wingless (wg)-GAL4	ventral thoracic disc, wing disc, haltere disc	embryonic-adult	Larval lethal (22-25°C)	Lethal: larval at 25°C, pupal at 22°C

* pupal lethal at higher expression with escapers

expression-dependent defects with more severe phenotypes at higher temperatures

** likely lethal at 18°C but CyO phenotype on balancer was suppressed so difficult to define flies with desired genotype

Figure S1: *dTnpo* RNAi cause tissue-specific phenotypes, including disruptions in animal, wing, and eye development. (**A**) *UAS-dTnpo RNAi* were ubiquitously expressed in L2-L3 larvae using *da-GAL4*. qPCR was used to define *dTnpo* mRNA levels. Animals were raised at room-temperature (~22°C). Statistics: 1-way ANOVAs with Dunnett's multiple comparisons test. P-value **<0.01. Error bars denote SD. Each dot represents the mean from replicate wells per sample. The mean from 3-4 individual samples is shown. **(B)** Ubiquitous expression of *dTnpo* RNAi using *da-GAL4* at 25°C causes lethality in larval stages. **(C)** Expression of *dTnpo* RNAi using *nub-GAL4* causes lethality with RNAi-1 and robust morphologic defects with RNAi-2. **(D)** Expression of *dTnpo* RNAi using *ey-GAL4* causes lethality with RNAi-1 and robust morphologic defects with RNAi-2, including a small eye and a rough eye phenotype. **(E)** Expression of *dTnpo* RNAi-1 in later stages of eye development using *GMR-GAL4* does not dramatically alter the external eye. *dTnpo* RNAi-2 expression causes a mild reduction in eye size. **(F)** Table summarizing the impacts of expressing *dTnpo*-targeting RNAi in different fly tissues and at different temperatures under control of the *GAL4/UAS* system. Red indicates conditions where the *dTnpo* RNAi disrupts expected "control" phenotypes. RNAi lines: "Control RNAi" is *UAS-Luciferase RNAi* (TRiP.JF01355), *UAS-dTnpo RNAi-1* is TRiP.HMJ23009, and *UAS-dTnpo RNAi-2* is KK108990.

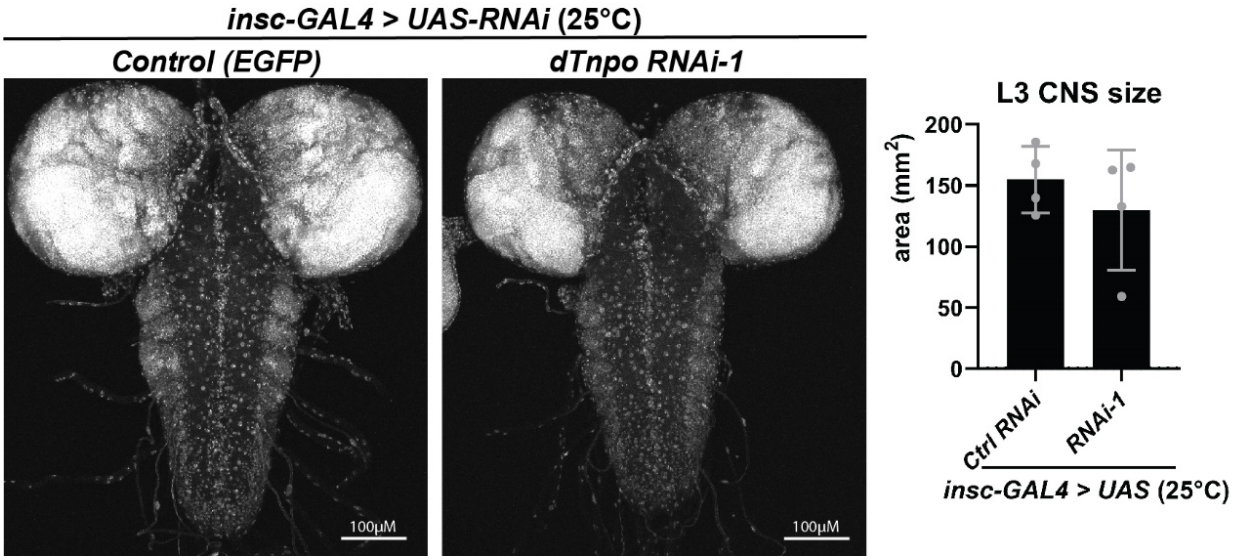

Figure S2: *dTnpo* RNAi expression in neuroblasts does not significantly reduce L3 CNS size. Expression of *dTnpo* RNAi in neuroblasts of the developing brain using *insc-GAL4* did not significantly alter the size of L3 CNS when compared to animals expressing a control RNAi targeting EGFP. Animals were raised at 25°C and CNS were dissected from wandering L3 animals right before pupariation as previously described[5]. Brains were counterstained with DAPI for imaging. The tissue area was measured from the 2-dimensional, Z-stacked images. Statistics: student t-test. Error bars denote SD. Each dot represents the area of the CNS from one animal.

A **Stage of death for *dTnpo* mutant flies expressing hTNPO2**

25°C	*dTnpo CRIMIC* (T2A-GAL4) > UAS						
	UAS Control	*hTNPO2*					
		WT	*p.Gln28Arg*	*p.Asp156Asn*	*p.Trp370Cys*	*p.Ala546Val*	*p.Trp727Cys*
dTnpo CRiMIC/ dTnpo[Gly736Asp]	L3*	L2*	L2*	L2*	L3*	L3*	L2*

*in rare cases puparia could be observed

B **Observed Mendelian ratios**

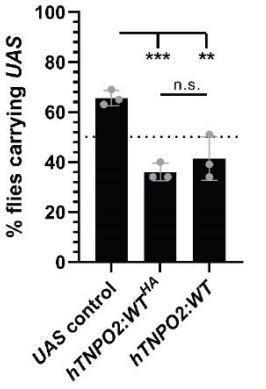

da-GAL4 x *UAS/Balancer* (25°C)

C **Summary of effects when *UAS-hTNPO2* lines are expressed in different tissues**

GAL4 Driver	Primary Tissue(s)	Stage	*UAS-hTNPO2*						
			WT ^{HA}	*p.Gln28Arg*	*p.Asp156Asn*	*p.Trp370Arg*	*p.Trp370Cys*	*p.Ala546Val*	*p.Trp727Cys*
Summary of variant impact versus wild-type hTNPO2									
Variant toxicity versus hTNPO2:WT^{HA}				↑↑↑	↑↑↑	↓↓	↓↓	↓	↓↓↑
Location in hTNPO2 protein				**RAN binding**		**Acidic loop**		**Cargo binding**	
Ubiquitous expression									
daughterless (da)-GAL4	ubiquitous	embryonic-adult	48% lethal at 25°C (p=0.001) vs UAS control; no significant lethality at 22°C	97% lethal at 25°C (p<0.0001) vs UAS control; 91% lethal at 22°C* (p<0.0001) vs UAS control	75% lethal at 25°C (p<0.0001) vs UAS control; 39% lethal 22°C* (p=0.04) vs UAS control	31% lethal at 25°C (p=0.01) vs UAS control; no significant lethality at 22°C	31% lethal at 25°C (p=0.01) vs UAS control; no significant lethality at 22°C	50% lethal at 25°C (p<0.0001) vs UAS control; no significant lethality at 22°C	no significant lethality at ≥22°C vs UAS control
Expression in the developing eye									
eyeless (ey)-GAL4	early eye development	embryonic-adult	phenotype at 29°C; rare phenotypes at ≤25°C	phenotypes at 29°C common; rare phenotypes at ≤25°C	phenotypes at 29°C common; rare phenotypes at ≤25°C	rare phenotypes ≥22°C	rare phenotypes ≥22°C	phenotypes at 29°C common; rare phenotypes at ≤25°C	some phenotypes at 29°C; rare phenotypes at ≤25°C
GMR-GAL4 (Glass)	late eye development, retina, some L3 brain expression	3rd instar-adult	mild rough eye phenotype 25°C; no phenotype at 22°C	rough eye phenotype ≥22°C	lethal at 25°C; rough eye phenotype at 22°C	mild rough eye phenotype 25°C; no phenotype at 22°C	mild rough eye phenotype 25°C; no phenotype at 22°C	mild rough eye phenotype 25°C; no phenotype at 22°C	mild rough eye phenotype ≥22°C
Expression in the developing wing									
nubbin (nub)-GAL4	ventral thoracic disc, wing disc, haltere disc	embryonic-adult	blister wing phenotype: 100% penetrant at ≥25°C, 50% penetrant at 22°C; minor gain-of-vein phenotype at 22°C; no serration at 22°C	blister wing phenotype: 100% penetrant ≥25°C, 99% penetrant at 22°C; minor gain-of-vein phenotype at 22°C; prominent serration at 22°C	lethal at 29°C; blister wing phenotype: 100% penetrant in escapers at 25°C, 98% penetrant at 22°C; moderate serration at 22°C (gain-of-vein not assessed)	blister wing phenotype: 100% penetrant at ≥25°C, 26% penetrant at 22°C; minor gain-of-vein phenotype at 22°C; no serration at 22°C	blister wing phenotype: 100% penetrant at ≥25°C, 14% penetrant at 22°C; minor gain-of-vein phenotype at 22°C; no serration at 22°C	blister wing phenotype: 70% penetrant at ≥25°C, 1% penetrant at 22°C; minor gain-of-vein phenotype at 22°C; no serration at 22°C	blister wing phenotype: 100% penetrant at ≥25°C, 65% penetrant at 22°C; moderate gain-of-vein phenotype at 22°C; rare serration at 22°C

* flies came up later – delayed development?

Figure S3: Extended *UAS-hTNPO2* data. (A) Expression of hTNPO2 cannot rescue lethality in *dTnpo* trans-heterozygote loss-of-function mutant animals. *UAS-hTNPO2* transgenes were expressed in the same spatiotemporal pattern as *dTnpo* using the *dTnpo CRIMIC (T2A-GAL4)* allele. Animals were trans-heterozygous for the hypomorph alleles, *dTnpo[Gly736Asp]* and *dTnpo CRIMIC*. Shown is data at 25°C while data obtained at 18°C and 22°C were consistent with these results. (**B)** The HA-tag in *hTNPO2:WT* does not significantly alter its function based on toxicity expected by calculating Mendelian ratios. 1-way ANOVA with Tukey's multiple comparisons test. P-values: **<0.01, ***<0.001. Error bars denote SD. Each dot represents one independent cross with >100 animals scored. The mean from three independent crosses is shown. **(C)** Table summarizing the impacts of ectopically expressing *UAS-hTNPO2* lines in different fly tissues and at different temperatures under control of the *GAL4/UAS* system. Red and orange indicate more severe phenotypes occur when compared to $hTNPO2{:}WT^{HA}$, with red highlighting when stronger impacts are observed. Green indicates a less severe phenotype occurs when compared to $hTNPO2{:}WT^{HA}$. Black indicates phenotypes that are similar to $hTNPO2{:}WT^{HA}$.

Fly Line	Genotype	Source
dTnpo RNAi-2 (used in [6])	*w*;; P{KK108990}VIE-260B*	VDRC #105181
dTnpo RNAi-1	*y[1] v[1]; P{TRiP.HMJ23009}attP40;*	BDSC #61230
Control (Luciferase) RNAi	*y[1] v[1];; P{y[+t7.7] v[+t1.8]=TRiP.JF01355}attP2*	BDSC #31603
Control (EGFP) RNAi	*y[1] sc[*] v[1] sev[21]; P{y[+t7.7] v[+t1.8]=VALIUM22-EGFP.shRNA.1}attP40*	BDSC #41557
ey-GAL4 (on II)	*w[*]; P{w[+m*]=GAL4-ey.H}3-8;*	BDSC #5534
GMR-GAL4 (on II)	*w[*]; P{w[+mC]=GAL4-ninaE.GMR}12;*	BDSC #1104
da-GAL4 (on III)	*w[*];; P{w[+mW.hs]=GAL4-da.G32}UH1, Sb[1]*	BDSC #55851
nub-GAL4 (on II)	*w[*]; P{w[nub.PK]=nub-GAL4.K}2;*	BDSC #86108
insc-GAL4 (on II)	*w[*]; P{w[+mW.hs]=GawB}insc[Mz1407]*	BDSC #8751
elav-GAL4^{GS} (on III)	*y[1] w[*];; P{w[+mC]=elav-Switch.O}GSG301*	BDSC #43642
ey-FLP, GMR-lacZ;; RpS17[4], w+ FRT80B	*y[d2] w[1118] P{ry[+t7.2]=ey-FLP.N}2 P{5xglBS-lacZ.38-1}TPN1;; RpS17[4] P{w[+t*] ry[+t*]=white-un1}70C P{ry[+t7.2]=neoFRT}80B/TM6B, P{y[+t7.7] ry[+t7.2]=Car20y}TPN1, Tb[1]*	BDSC #5621
Ubx-FLP	*y[1] w[*] P{w[+mC]=Ubx-FLP}1;;*	BDSC #42718
Ubi-GFP FRT80B	*w[*];; P{w[+mC]=Ubi-GFP.D}61EF P{ry[+t7.2]=neoFRT}80B*	BDSC #1620
UAS-mCherry.NLS (on III)	*w[*];; P{w[+mC]=UAS-mCherry.NLS}3*	BDSC #38424
UAS-mCD8::RFP (on II)	*w[*]; P{y[+t7.7] w[+mC]=10XUAS-IVS-mCD8::RFP}attP40;*	BDSC #32219
Df(3L)Exel8101	*w[1118];; Df(3L)Exel8101/TM6B, Tb[1]*	BDSC #7928
UAS::dTnpo^{GS11030}	*y[1] w[67c23];; P{GSV6}Tnpo[GS11030]/TM3, Sb[1] Ser[1]*	Kyoto #205260

Table S1: Publically available fly lines used in this study.

Assay	Name	Species	Forward primer (5'-3')	Reverse primer (5'-3')
Q5 mutagenesis	*TNPO2:stop*	Hsap.	tagGACCCAGCTTTCTTGTACAAAG	GACCCCATAGAAAGCCGC
	TNPO2:p.Gln28Arg	Hsap	ACAGCCACTCgGCGCATCGTG	GTTGGGCGACTGTGAGTCTTTG
	TNPO2:p.Asp156Asn	Hsap	GATCTGTGAAaACTCATCAGAGC	TTCTGCAGGGCTCCAAAG
	TNPO2:p.Trp370Cys	Hsap	TCTGTCCGACcGGAATTTGAG	GCATCATCATCATCGTCATC
	TNPO2:p.Trp370Arg	Hsap	TGTCCGACTGcAATTTGAGGAAG	GAGCATCATCATCATCGTC
	TNPO2:p.Ala546Val	Hsap	GGCACCCTGGtCGACTCTGTA	AATGGCGTCATAGAGGATGAGC
	TNPO2:p.Trp727Cys	Hsap	ACGCCACCTGtGCCATTGGTG	TGTTGCAGACGGAGATGAAC
Sequencing	*TNPO2* cDNA primer 1	Hsap	CACTGCAGTCCCAAGATCC	n/a
	TNPO2 cDNA primer 2	Hsap	TCCTCGCCAATGTCTTCC	n/a
	TNPO2 cDNA primer 3	Hsap	CCTGCTGGAGTGTCTGTCAT	n/a
qPCR	*Tnpo* (1:10)	Dmel.	GCCCGAATTTGTACGACAGT	GCAGATCCTCTGGTGGGTTA
	RP49 (1:100)	Dmel.	TGTCCTTCCAGCTTCAAGATGACCATC	CTTGGGCTTGCGCATTTGTG
	RPS20 (1:100)	Dmel.	CCGCATCACCCTGACATCC	TGGTGATGCGAAGGGTCTTG
	Tubulin (1:20)	Dmel.	CATCCAAGCTGGTCAGTG	GCCATGCTCATCGAGAT

Table S2: Primers used in this study.

REFERENCES

1. Coe, B.P., Witherspoon, K., Rosenfeld, J.A., van Bon, B.W.M., Vulto-van Silfhout, A.T., Bosco, P., Friend, K.L., Baker, C., Buono, S., Vissers, L.E.L.M., et al. (2014). Refining analyses of copy number variation identifies specific genes associated with developmental delay. Nature Genetics *46*, 1063–1071.

2. Lehman, A.M., McFadden, D., Pugash, D., Sangha, K., Gibson, W.T., and Patel, M.S. (2008). Schinzel-Giedion syndrome: report of splenopancreatic fusion and proposed diagnostic criteria. Am J Med Genet A *146A*, 1299–1306.

3. Barington, M., Risom, L., Ek, J., Uldall, P., and Ostergaard, E. (2018). A recurrent de novo CUX2 missense variant associated with intellectual disability, seizures, and autism spectrum disorder. European Journal of Human Genetics *26*, 1388–1391.

4. Lindstrand, A., Grigelioniene, G., Nilsson, D., Pettersson, M., Hofmeister, W., Anderlid, B.-M., Kant, S.G., Ruivenkamp, C.A.L., Gustavsson, P., Valta, H., et al. (2014). Different mutations in PDE4D associated with developmental disorders with mirror phenotypes. J Med Genet *51*, 45–54.

5. Link, N., Chung, H., Jolly, A., Withers, M., Tepe, B., Arenkiel, B.R., Shah, P.S., Krogan, N.J., Aydin, H., Geckinli, B.B., et al. (2019). Mutations in ANKLE2, a ZIKA Virus Target, Disrupt an Asymmetric Cell Division Pathway in Drosophila Neuroblasts to Cause Microcephaly. Developmental Cell *51*, 713-729.e6.

6. Shi, Q., Han, Y., and Jiang, J. (2014). Suppressor of fused impedes Ci/Gli nuclear import by opposing Trn/Kapβ2 in Hedgehog signaling. J Cell Sci *127*, 1092–1103.